X-612-66-530

MAGNETIC FIELD MEASUREMENTS WITH THE IMP II SATELLITE

BY
D. H. FAIRFIELD
N. F. NESS

NOVEMBER 1966

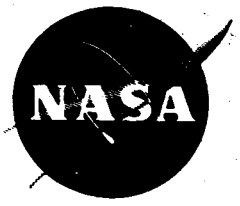

GODDARD SPACE FLIGHT CENTER
GREENBELT, MARYLAND

MAGNETIC FIELD MEASUREMENTS WITH THE IMP 2 SATELLITE

by

D. H. Fairfield*

and

N. F. Ness

NASA-Goddard Space Flight Center
Greenbelt, Maryland

---

*NAS-NASA Resident Research Associate at Goddard Space Flight Center, Greenbelt, Maryland

ABSTRACT

The IMP 2 satellite was launched on October 4, 1964 with apogee at 15.9 R_E near the Earth-Sun line. Two onboard monoaxial fluxgate magnetometers measured magnetic fields in interplanetary space, the magnetosheath, and the magnetosphere during the time interval between launch and April 7, 1965. Analysis of over 325 hours of interplanetary data distributed throughout the first two months of operation revealed structuring of the interplanetary magnetic field into four recurring sectors of approximately equal size. Average fields within each sector were directed either toward or away from the sun near the theoretical spiral angle. High magnitudes and increased geomagnetic activity tended to occur early in the sectors and lower fields and quiet conditions at the end. Field directions in the magnetosheath were found to be highly dependent on the sector direction. Results suggest that fields convected through the bow shock front undergo compression and an angle change at the shock and subsequently tend to become aligned tangent to the magnetopause. Frequently both the shock front and the magnetopause were observed to move back and forth past the satellite. Comparisons with onboard plasma detectors showed very good agreement in identifying the magnetosheath. Several passes were notable for the lack of a clear magnetopause in both plasma and field data. The average magnetic field topology in the magnetosphere between approximately 9 and 16 R_E in the dawn-to-midnight region was definitively mapped. Results demonstrate solar wind distortion of the magnetosphere and the gradual formation of the magnetic tail in the dawn-to-midnight region.

I. INTRODUCTION

The IMP 2 or Explorer 21 spacecraft was launched from Cape Kennedy, Florida, at 0345 GMT on October 4, 1964. The apogee at launch was in the sunward direction at a geocentric distance of 101,940 Km = 15.9 R_E (earth radii) and the perigee was 197 Km above the surface of the earth. Initially the orbit was inclined to the geographic equator at an angle of 33.5° and the orbital period was 34.9 hours. The apogee was 5.6 R_E below the solar ecliptic plane at launch but six months later it had changed to 3 R_E below. The spacecraft was spin stablilized with an initial spin rate of 14.58 rpm which subsequently increased to 18 rpm due to solar radiation pressure acting on the solar paddles. The spin axis direction in celestial inertial coordinates at launch was right ascension = 41.4°, declination 47.4°, and had changed to right ascension = 76°, declination = 22° near the end of the productive lifetime on April 7, 1965.

A malfunction in the third stage of the launch vehicle was responsible for the IMP 2 apogee being less than one-half the intended value and for the spin rate being well below the 23 rpm nominal value. Also, the spin axis direction was 78° removed from its nominal pre-launch value, which led to an unusually wide range of incident sun angles, causing overheating and a partial failure of the silver-cadmium battery after two months operation. Thereafter power was obtained directly from the solar paddles and operation was limited to times of favorable sun aspect angle relative to the spin axis.

In figure 1, the orbit of IMP 2 is shown projected on the solar ecliptic plane with the sun toward the left. As the earth progresses around the sun, the orbit appears to move by 1.5° per orbit toward the dawn meridian.

During the first 40 orbits from October 4 to November 30, 1964 the spacecraft mapped the earth's magnetopause and penetrated through the bow shock wave into the interplanetary medium on almost every orbit. During the 12 orbits from November 31 to December 17, 1964 unfavorable sun angles and a failing battery resulted in intermittant operation. On December 18, during orbit 53 the sun angle had changed so that nearly continuous operation was again possible until orbit 89 in February 1965. During this interval the spacecraft continued mapping the magnetopause and making measurements in the magnetosheath and the magnetosphere. On February 9, 1965, the incident sun angle again reached a value such that solar paddle power was inadequate and operation became erratic until March 6, 1965. Useful data was obtained from orbits 107 through 128 but after April 7, 1965 only very short intervals of data were obtained.

Officially IMP 2 was designated a failure because its low apogee precluded extended observations of the interplanetary medium. In practice considerable data on magnetic fields were obtained in the magnetosphere, the magnetosheath and even for a limited time in interplanetary space. This paper summarizes the general results obtained by the magnetic field experiment.

Because of the intermittent operation and continually varying spin axis, an extensive analysis has been performed on the data obtained from the magnetic field experiment in order to verify its accuracy. This work is discussed in Sections 2 and 3. Measurements of the magnetosheath and its boundaries are discussed in section 4, and motion of both of these boundaries is emphasized. Interplanetary magnetic field measurements are presented in section 5, and the sector structure of the interplanetary

field is discussed and related to other satellite measurements at different epochs. In section 6 the topology of the geomagnetic field in the dawn-to-midnight region is presented. Reports by Wolfe et al. (1966), Serbu and Maier (1966), Balasubrahmanyan et al.(1965), and Anderson (1965) have discussed limited results obtained from other experiments on the same satellite.

2 INSTRUMENTATION AND ANALYSIS

Both the instrumentation of the magnetic field experiment and the satellite data telemetry format on IMP 2 are identical to that of IMP 1 flown one year earlier (Ness et al.,1964). Two monoaxial fluxgate magnetometers (hereafter referred to as A and B) were mounted at the extremities of double sectioned folding booms. These booms were erected at third stage separation so that the sensors were placed 2.1 meters from the center of the spacecraft.

The sensors make nominal angles of 60° and 30° respectively with the spacecraft spin axis and have dynamic ranges of approximately $\pm$ 40 gammas. Magnetic fields greater than 40 gammas can be measured, depending on the angles the detector and the field direction make with the spin axis. IMP 2 also carried a rubidium vapor magnetometer with a range of 3-500γ. This instrument operated intermittently because of poor signal-to-noise ratio during early orbits but produced some useful total field measurements later in the flight.

The telemetry data format on IMP 2 is based on a sampling cycle which repeats every 5.46 minutes. During this interval the two fluxgate magnetometers are alternately sampled continuously for 4.8 seconds at 20.5 second intervals until 12 measurements have been obtained. Then the rubidium vapor magnetometer is sampled continuously for 81.9 seconds before the fluxgates are again sampled at the beginning of the next cycle. Each 4.8 second data sample is the spin modulated output of one of the fluxgate sensors. The telemetry data is digitized on the ground with $\pm$0.4 gamma precision at intervals of 0.160 seconds. A ten gamma calibration field is added to the ambient field

during the first four data points and the vector field information is extracted from the remaining 26 sample points. This spin modulated curve from IMP 1 was analyzed with numerical filters but the abnormally low spin rate of IMP 2 made an alternate approach necessary.

The new method chosen was to obtain the best fit sinusoid to the 26 data points by minimizing the square of the deviations of the assumed sine wave from the actual curve. The spacecraft spin rate is measured from the onboard solar aspect sensor, so the parameters to be determined in the least squares fitting are the sinusoid amplitude A, the zero base level C, and the phase ϕ_o. The detected output D is the component of the field $\vec{B}$ parallel to the sensor $\vec{S}$ and may be written as

$$D = \vec{B}\cdot\vec{S} = B\cos\alpha\cos\theta + B\sin\alpha\sin\theta\cos(\omega t - \psi) = C + A\cos(\omega t - \phi_o) \quad (1)$$

where α is the angle betwee $\vec{B}$ and the spin axis, ψ is the aximuthal angle of the field relative to the satellite-sun vector, θ is the angle the sensor makes with the spin axis, and ω is the spin frequency.

The first term is the field along the spin axis projected on the detector and is independent of time. This term can be identified as the zero level of the curve, so $B\cos\alpha = B_{//} = \frac{C}{\cos\theta}$. The second term in equation 1 is the field perpendicular to the spin axis projected on the detector. This term varies with time as the detector spins and the coefficient of $\cos(\omega t - \psi)$ may be equated to A, the amplitude of the curve. Thus $B\sin\alpha = B_{\perp} = \frac{A}{\sin\theta}$. The quantities $B_{//}$, $B_{\perp}$ and ψ completely determined the vector field in payload coordinates. Rotation into more meaningful coordinate systems can be accomplished with knowledge of the spin axis direction.

The accuracy of the vector measurement determined by a single spinning sensor may be poor if the ambient field fluctuates during the 4.8 second sampling interval. To check on the quality of the fitted curves, the root mean square deviation of the 26 data points from the Least Squares curve was computed. A good fit to the data points is then an indication of the relative unimportance of the time variations in the field.

Figure 2 shows four examples of raw spin modulated data with computer determined best fit curves and associated root mean square deviations Δ. The lower right hand curve illustrates typical interplanetary data, the value of Δ=.3 gamma being typical of interplanetary space. It is essentially the noise level of the instrument due to the $\pm$ 0.4 gamma digitization of the data processing procedure. The three remaining panels in Figure 2 illustrate data from the magnetosheath. The upper right hand curve with Δ = 0.6 is representative of a relatively good fit in the magnetosheath while the remaining two curves with Δ = 1.6 and 1.5 gammas are relatively poor fits. This parameter Δ is essentially a measure of field fluctuations with periods less than 4 seconds and has proven very useful in the data analysis, particularly in defining the earth's bow shock front. An example of this will be presented in section 4.

As a check on the accuracy of the vector measurements of the monoaxial spinning magnetometers, the quantity $\frac{\Delta}{B}$ was investigated in the magnetosheath

and in interplanetary space during the first 40 orbits. Large values (>0.5) of this quantity indicate significant distortion of the assumed sinusoid and possibly inaccurate vector measurements, while small values indicate reliable measurements. Results showed an average value of $\Delta/B = 0.12$ in the magnetosheath and $\Delta/B = 0.09$ in interplanetary space during the first 40 orbits. The largest orbit average was 0.20 for the magnetosheath and 0.17 for interplanetary space with the smallest orbit average being 0.05 for both magnetosheath and interplanetary. On all but five orbits more than half the individual measurements in the magnetosheath have $\frac{\Delta}{B}$ less than 0.1. On all but one of these orbits three quarters of the measurements had $\frac{\Delta}{B} < 0.2$. The quantity $\frac{\Delta}{B}$ in interplanetary space is smaller than in the magnetosheath in spite of the smaller B values. In the magnetosphere $\frac{\Delta}{B}$ was not calculated but would be considerably smaller than in the magnetosheath, since Δ tends to be smaller and B larger.

These very small values of $\frac{\Delta}{B}$ demonstrate that the accuracy of the monoaxial spinning fluxgate magnetometer is not seriously impaired even by the "turbulent" fields of the magnetosheath. It should be noted that the values of $\frac{\Delta}{B}$ where Δ is calculated from 4.8 seconds of data is considerably smaller than the quantity $\frac{\delta Xi}{B}$ previously reported (Ness et al, 1964) where δX is calculated from the 12 vector samples calculated every 5.46 minutes. Interpretation of this result in the context of the frequency spectrum of the magnetic fluctuations leads to the conclusion that there is significantly more energy in the fluctuations with periods of minutes than in fluctuations with periods of seconds.

3 IMP 2 DATA CORRECTIONS

Initial inspection of the IMP 2 data in payload coordinates revealed discrepancies in the vector fields measured by the two fluxgates. These discrepancies may be related to the third stage misfire and subsequent mechanical and electrical stresses. Three types of corrections necessary to bring the data into agreement are described in this section. An estimate of the possible uncertainties in the corrected fields is made after an investigation of the maximum magnitude of the corrections and their uncertainties.

The most obvious of the discrepancies between the fluxgates was a difference of approximately 10γ in the component parallel to the spin axis. This effect can be attributed to erroneous pre-flight calibration, instrumental drift in the sensor zero levels, and/or spacecraft magnetic field. Further inspection of the data revealed a difference in the perpendicular field components measured by the two fluxgates. This difference varied with magnitude and was accompanied by a somewhat smaller magnitude-dependent difference in the parallel components superposed on the 10γ offset mentioned above. These magnitude dependent differences cannot be due to a zero offset, and and therefore have been interpreted as misalignment of the spin axis-sensor angle θ which could be due to incomplete or improper boom extension.

To obtain detailed information on the magnitudes of these discrepancies and their variations throughout the spacecraft lifetime, ten minute averages of the perpendicular and parallel components were computed independently for each fluxgate. Quiet field intervals, generally of several hours length, were processed on approximately one-third of all the orbits. These results indicated that the perpendicular components differed by 15 $\pm$ 2 percent

from each other at the beginning of the lifetime, with differences decreasing to 5 ± 2 percent near the end of the lifetime. The magnitude independent part of the parallel component difference was found to be 9γ shortly after launch, with an increase to 11γ near orbit 70 and a decrease to 9γ late in the lifetime. The precision of these corrections is estimated as ±½γ in the quiet interplanetary and magnetosphere fields and ±½γ in the noisier fields near the middle of the lifetime. The magnitude dependent part of the parallel differences are 10 ± 3 percent shortly after launch and near zero late in the lifetime.

A third correction was based on a check of the on-board calibration field. During the first 40 orbits this field was found to be within 0.2γ of its nominal 10γ value for each fluxgate. After the first turn-off of the satellite, fluxgate A calibration increased gradually to 11 ± .1γ and fluxgate B increased to 10.5 ± .1γ. In accord with this information the total field magnitudes for fluxgates A and B were reduced by a maximum of 10 and 5 percent respectively depending on the particular orbit.

The application of the zero offset correction was not as straightforward as the sensitivity correction, since it was not known unambiguously which of the two fluxgates was in error or if both were in error. It was immediately obvious, however, most of the 10γ error had to be attributed to fluxgate A in order that the interplanetary fields (known to have typical magnitudes of five gammas and to vary appreciably in direction over long time intervals) not have inordinately high values and always point generally along the spin axis. Further evidence that the offset was in fluxgate A was obtained by sampling the parallel field components randomly throughout the first 24 orbits. The average for fluxgate

A was 9.0γ while the average for B was -.1γ. Interplanetary fields on the average are known to have a small component perpendicular to the ecliptic plane (Ness and Wilcox, 1964) and the spin axis of IMP-2 was roughly perpendicular to the ecliptic plane early in the lifetime. Therefore, an average parallel component near zero might be expected. On the basis of this evidence the entire difference was attributed to fluxgate A during the first 89 orbits and the appropriate correction was applied. After the spacecraft turn-off period in orbit 89 an additional three gammas was subtracted from each fluxgate to improve the agreement with the Rubidium vapor magnetometer measurements of the steady fields of the tail region. This additional error may be due either to instrumental drift or analog oscillator drift.

A different type of correction has been applied to remove the magnitude-dependent discrepancy between the two fluxgates. This correction takes the form of a modification to the spin axis-detector angle θ which changes the field in accord with the equations in the previous section. Once the differences between the fluxgates have been determined, the θ's required to make the fluxgates agree are uniquely determined. These corrected θ's range from 63° to 66° for fluxgate A (nominal value 60°) and 34° to 38° for fluxgate B (nominal value 30°).

During the latter half of the IMP 2 lifetime, the spacecraft traversed the dawn-to-mignight portion of the magnetosphere where the fields are below the fluxgate saturation level and also tend to be very steady. In these regions, total field measurements were available from the rubidium vapor magnetometer for comparison with the fluxgate measurements. These comparisons show that the corrections applied to the fluxgate data improve

the agreement between the two instruments, yet differences of up to 3 or 4 gammas in fields of 40 gammas still exist. Therefore, it appears that despite the fact that the two fluxgates can be brought into very good agreement with one another, the absolute values of magnitude and direction may be in error. An upper limit on the magnitude of these errors can be estimated after investigating the magnitude of the corrections and their probable uncertainties.

The most straightforward correction is that arising from the on-board sensitivity check. This correction was not necessary during the first 40 orbits, and later was a maximum of ten percent of the total field for fluxgate A and 5 percent for fluxgate B. This correction is a simple reduction in total magnitude, which does not alter the field direction.

The angular (θ) correction affects the parallel and perpendicular components by different amounts and hence affects the field direction as well as the total magnitude. The maximum change in magnitude due to angular corrections is a 22% increase in fluxgate A field magnitude when the field is perpendicular to the spin axis. The largest change in direction due to this type correction is about 8^{o} and occurs when the field makes an angle near 45^{o} with the spin axis.

The effect of the parallel offset correction will depend strongly on the total magnitude of the field. For weak ambient fields subtraction of a constant parallel offset may dominate the ambient field and cause very large angle changes. On the basis of the weak field interplanetary measurements early in the lifetime and the Rubidium vapor magnetometer comparisons later in the lifetime, it is clear that the uncertainty in the

parallel offset is less than the 10-12γ correction that was made. A conservative estimate to the uncertainty of this correction may be taken as $\pm 3\gamma$. During early orbits in interplanetary space this uncertainty is more like $\pm 1\gamma$. Fields less than 10γ are seldom measured by IMP-2 during the later period when the spacecraft is in the magnetosheath and the magnetosphere. For this ten gamma field a three gamma change in the parallel component can produce a 30% change in magnitude when the field is parallel to the spin axis and an 18° change in angle when the field is nearly perpendicular to the spin axis.

It should be emphasized that the corrections discussed above are generally the largest corrections that were applied to the data under field conditions that maximize the magnitude of the correction. At many periods throughout the lifetime the maximum corrections made are not this large. It is not possible to estimate the uncertainties in these corrections and arrive at specific fixed limits on the absolute accuracy of IMP-2 measurements. The best conservative estimate on the accuracy of the absolute magnitudes may be taken as 10% except in small fields (< 10 gammas) where it may be somewhat larger. For the absolute value of the field direction the uncertainty is $\pm 8^{\circ}$, except in the very small fields when it is somewhat larger.

SECTION 4. THE MAGNETOSHEATH AND ITS BOUNDARIES

The magnetosheath of the earth, where shock-disturbed solar plasma flows around the magnetosphere, has been traversed by numerous satellites in recent years. (See Review by Ness, 1966). The average positions of the inner boundary of this region, the magnetopause, and the outer boundary, the collisionless shock front, have been mapped near the solar ecliptic equatorial plane for a wide range of local times and solar conditions. This section presents results of measurements made by the IMP-2 satellite in this region.

Figure 3 illustrates the results of orbit 4 in a form similar to that used by Ness et al. (1964) on IMP 1. Each point is the average of 12 measurements made over an interval of 5.46 minutes. The fields are given in terms of the magnitude, F, and latitude and longitude angles θ and ϕ in a solar ecliptic coordinate system. The rms deviations of the 12 measurements along each axis has been computed, although only δX is shown as representative of the three axes.

At the bottom of figure 3 are negative current values from the plasma detector of G. P. Serbu of GSFC on board the same spacecraft. This retarding potential plasma analyzer alternately sweeps the ranges $\mp .5$ to $\pm$ 15 and $\mp$ 5 to $\pm$ 45 volts and has been described elsewhere (Serbu and Maier, 1966). Only net negative currents are shown here and the values (in amperes) are the approximately constant values obtained when the retarding potential is more negative than -5 volts. The solid circles designate values computed for the -5 to -45 volt range and open circles for the -5 to -15 volt range. The open circles computed for the more limited range have been used only when the greater range measurements were unavailable.

Figure 3 covers the interval beginning when IMP-2 is outbound from inside the magnetosphere and terminating with the spacecraft again inside the magnetosphere on the inbound pass. A readily identified magnetopause crossing is evident at 10.5 R_E, where all the field quantities exhibit discontinuous changes. The electron current also rises near the magnetopause and remains high until the spacecraft approaches the shock front at 2115 on October 8, 1964. After an interval of low field magnitude, RMS deviation and negative current typical of interplanetary space, the field magnitude exhibits another increase at 0035 on October 9. During the following hour, the field magnitude and electron current show values typical of the magnetosheath but δX, as well as the parameter Δ (not shown), have unusually small values.

Two interpretations of this event are possible. One is that the shock front has moved out past the satellite at 0035 with the outbound satellite overtaking the shock at 0140. The second is that incoming solar wind with enhanced field and plasma has passed by the satellite at this time. The former explanation appears most plausable since similar events are frequently observed near the shock front on IMP-2 whereas these types of events have not been observed on satellites such as IMP-1 far from the shock front. The low level of field disturbance at this time is unusual for the magnetosheath, but other periods in the magnetosheath almost as quiet have been observed. Observations of motion of the shock have also been reported by Holzer et al. (1966) and Bridge et al. (1964).

Continuing inbound the satellite encounters another shock crossing near $\sim$15 R_E followed by the magnetopause crossing just outside 12 R_E. It should be noted that the inbound crossings are about 2 R_E further out than the outbound crossings in spite of the fact that inbound crossings are

slightly nearer the earth-sun line where they would normally be expected to be closer. This shows that boundaries may move appreciably over a time interval of several hours. Subsequent figures will emphasize the importance of the motion of boundaries on shorter time scales.

Figure 4 presents the data for orbit 22 on November 3-4, 1964. Again during orbit 22 there is a high field region near apogee which displays all the characteristics of the magnetosheath. This is almost certainly a case of the shock moving out past the spacecraft and immersing the spacecraft in the magnetosheath. On this orbit the rms deviations δX as well as the field magnitude and electron current display typical magnetosheath values. The δX values in this figure also illustrate the various levels of field variability which are characteristic of the magnetosheath. On this orbit magnetosheath data from the outbound pass is relatively quiet while on the inbound pass the magnetosheath is considerably more turbulent.

The time interval 0000 to 0600 on November 4 in figure 4 is shown on an expanded time scale in figure 5. Here the field magnitude F and the parameter Δ (See section 2) are presented for each 4.8 second measurement. Four very sharp shock crossings are evident and labelled. A few points at 0215 are probably also associated with the shock. At times the field magnitude and parameter Δ change from low interplanetary values to high magnetosheath values from one individual measurement to the next. At other times such as SW1 in figure 5 the magnitude may change monotonically for several measurements. At still other times Δ may increase slightly in interplanetary space before the magnitude increases in its typically abrupt manner. This latter phenomena is equivalent to the detection of rapid fluctuations outside the shock reported by Heppner (1965) since Δ measures

the high frequency end of the spectrum. If one neglects these waves in the low-field-magnitude interplanetary region and defines the shock as the region of transition from undisturbed interplanetary conditions to higher field magnetosheath conditions, the transition can be said to usually occur over a time interval of less than 60 seconds. Often the transition clearly occurs between measurements separated by 20.5 seconds. Less frequently the variations in the interplanetary medium become greater before the magnitude increases and the shock becomes less clearly defined. Since the spacecraft is traveling at a velocity of less than 1 km/sec., the unknown velocity of the shock front is undoubtedly the most important factor in converting these transitions times to shock thicknesses. Detailed comparison with shock positions identified by the MIT plasma experiment (Binsack 1966) are in excellent agreement with the magnetic field shock identifications. On all orbits compared, the first appreciable deviation from interplanetary conditions corresponded to transition from directional interplanetary flow to more isotropic magnetosheath conditions.

Returning to Figure 4 it is of interest to examine the magnetopause in more detail. The outbound and inbound magnetopause crossings have been marked just outside $13R_E$ and inside $11R_E$ respectively but this is an over-simplification. On the outbound pass a detailed study shows that about 15 minutes after the crossing marked on figure 4 the magnetopause overtakes the outbound spacecraft so that the spacecraft spends about 5 minutes in the magnetosphere before again overtaking the magnetopause. On the inbound pass there are several multiple boundary crossings which are rather obscured in the 5 minute averages of figure 4.

This boundary motion phenomena is better illustrated in figure 6 which shows the individual 4.8 second measurements during the inbound pass of orbit 28. The dashed line represents the theoretical field determined from the Finch and Leaton (1955) coefficients and its presence corresponds to periods when the spacecraft is within the magnetosphere. Both experimental and theoretical fields are given in a coordinate system defined here as solar magnetic. The Z axis points along the dipole axis, the X axis lies in the plane formed by the Z axis and the earth-sun line, and the Y axis completes the right-handed orthogonal system. When the spacecraft is within the magnetosphere the measured field strength is approximately twice the theoretical field while the observed angles differ from the theoretical values in a manner which corresponds to enhanced compression near the equatorial plane and twisting of the field out of the meridian plane. (See section 6 for further discussion of the magnetospheric topology). After the initial magnetopause crossing at 0805 four different intervals are apparent when the spacecraft returns to conditions similar to those experienced before the initial magnetopause crossing. A typical magnetopause crossing occurs on a time scale of one minute and is probably somewhat longer than the typical shock crossing. This is in agreement with the results of Cahill and Amazeen (1963) where better time resolution permits the study of these phenomena more clearly.

Figure 7 illustrating orbit 19 shows clear magnetopause crossings near 12 R_E both outbound and inbound. Almost four continuous hours of interplanetary measurements are encountered on the inbound portion of this orbit. Additional shorter intervals of interplanetary field (not marked) can be easily discerned from detailed plots and are found to occur near 2015, 2100, 0255, 0315, 0430, and 0510.

Figures 8 illustrates orbit 8 and is of special interest because of the outbound traversal through the magnetopause. On this orbit there is no clear discontinuity in either field magnitude, direction or electron current. This has been observed to occur on occasional orbits and the lack of a clear magnetopause in the magnetic field data invariably corresponds to a diffuse plasma magnetopause characterized by slowly changing plasma currents (Binsack 1966). This phenomena has important implications concerning the entry of plasma into the magnetosphere and will be pursued in future work. On the inbound pass in figure 8 the field boundary is again very well defined by magnitude and angle discontinuities.

A summary plot showing intervals when IMP-2 was in the magnetosheath is presented in figure 9 which shows the solar ecliptic plane with the sun at the left. All spacecraft positions have been transformed into the solar ecliptic plane by rotating them in a meridian plane. The inner terminations of each orbit represent magnetopause crossings and the outer terminations represent shock crossings except when an arrowhead designates that data was missing and the boundary is beyond the end point. The occurrence of boundary motion is illustrated by breaks in the lines on many orbits although many short period boundary movements cannot be presented clearly in this type of presentation. Average positions of the shock and the magnetopause have been sketched on Figure 9 and are in good agreement with previous results (See review by Ness 1966).

The spacecraft penetrated the magnetopause on every orbit investigated prior to orbit 69 and again on orbits 70, 72, and 77. The closest magnetopause crossings observed by IMP-2 occurred at 8.9 R_E on the outbound pass of orbit 16 three minutes after the observation

of a sudden commencement geomagnetic storm (Lincoln 1965). On this same pass, the interplanetary field was encountered at 11 R_E which was the nearest to the earth that the interplanetary medium was observed. The outermost observation of the magnetosphere within 45° of the earth sun line occurred at 14.0 R_E on orbit 14. It is apparent in figure 9 that magnetopause crossings near the same meridian may vary by ± 2.5 R_E or more.

Another unusually close magnetopause crossing occurred on orbit 25 and was near the beginning of a magnetic storm. Additional evidence for compression at the time of storms comes from the outbound pass of orbit 30. On this orbit the spacecraft passed through the magnetopause near its average position of 12.5 R_E shortly before a sudden commencement storm. While the spacecraft was in the magnetosheath the sudden commencement storm occurred and the shock wave was observed only 72 minutes later, 0.8 R_E beyond the magnetopause crossing. The magnetopause crossing on orbit 77 occurred approximately 43 hours after a storm sudden commencement which occurred at 1612 on January 20. No magnetopause had been observed, however, when the spacecraft was at apogee on the previous orbit 14 hours after the sudden commencement.

Clearly the boundaries move in at the time of a storm sudden commencement although correlation between magnetopause position and Kp is not readily apparent. This lack of correlation is in agreement with results of Patel and Dessler (1966) and is probably related to inflation of the magnetosphere by the ring currents associated with enhanced magnetospheric plasma. (Freeman 1964). During the recovery phase of

magnetic storms there is some evidence from IMP 2 for larger magnetopause distances such as seen by Freeman on Explorer 12. The conclusion is that increased solar wind pressure is the important effect early in a storm producing a reduced boundary position. Later in a storm the internal pressure associated with inflation of the inner magnetosphere is dominant and leads to increased boundary distances. The anomalous case of orbits 76 and 77 may be related to dynamics of the storm associated with the tail and polar substorms.

SECTION 5. INTERPLANETARY MAGNETIC FIELDS

The IMP-2 mission was considered a failure due to the inability to make extended observations of the interplanetary medium. However, the satellite penetrated the bow shock and made interplanetary measurements for periods of 30 minutes to 20 hours per orbit on 35 of the first 40 orbits during solar rotations 1795-1797. Over 43,100 individual 4.8 second interplanetary measurements were obtained which is equivalent to more than 325 hours of data. The interplanetary measurements are often interspersed with intervals of magnetosheath data due to shock motion, but the clarity of the shock front has made it possible to isolate the interplanetary data for independent study.

The distribution of these individual field magnitudes is shown in figure 10. The relative number of occurrences in each 1/2 gamma interval is plotted versus magnitude. The average interplanetary field magnitude is seen to be between 5 and 6 gammas and the most probable value is around 4 gammas. It is likely that these measurements are not an exact representation of typical interplanetary field conditions since the availability of the measurements is dependent on the position of the shock which in turn is dependent on solar wind conditions.

Another important characteristic of the interplanetary magnetic field is its directional orientation over time intervals comparible to the 27 day solar rotation period. The IMP-1 satellite magnetic field data obtained near the end of 1963 revealed that the interplanetary magnetic field direction in the ecliptic plane was divided into four distinct sectors (Ness and Wilcox, 1965). Within each sector the field was directed predominantly toward or away from the sun near the theoretical spiral

angle predicted under the assumption of plasma flowing radially outward from a rotating sun. These satellite measurements correlated well with solar magnetograph observations of the sun's field and support the interpretation that the interplanetary field is connected to the sun (Ness and Wilcox, 1964). As the sun rotates these sectors were found to sweep past the earth, reappearing approximately every 27 days. Various other solar wind parameters, geomagnetic activity, and cosmic ray intensity were also found to be related to the sector structure, (Wilcox and Ness, 1965). IMP-1 measurements were limited to the study of three solar rotations in late 1963 - early 1964 and it is of interest to examine the structure of the interplanetary medium at other times.

Mariner 2, launched in August 1962, made interplanetary measurements during three solar rotations in late 1962 and found evidence for two sectors (Davis et al, 1966). Mariner 4 launched one year after IMP-1 made interplanetary measurements which have been reported for three solar rotations from December 1964 - February 1965 (Coleman et. al. 1966). These results indicated the presence of several sectors but they did not exhibit the well defined recurrence patterns of either Mariner 2 or IMP-1.

The procedure used for studying field directions on IMP-2 was to divide a sphere representing a solar ecliptic coordinate system into 96 equal solid angles. The distribution of individual 4.8 second interplanetary field measurements among these 96 equal solid angle regions was then investigated for each orbit. The division of the sphere was accomplished by first creating nine latitude regions bounded by the latitudes $\pm 78.3^{o}$, $\pm 54.3^{o}$, $\pm 34.2^{o}$, $\pm 10.8^{o}$. The polar regions above $\pm 78.3^{o}$ each formed one region. The region between 54.3^{o} and 78.3^{o} was divided into eight

intervals of 45° longitude, and lower latitude regions were divided into 12 or 18 intervals of 30° and 20° longitude. The 96 regions are projected on a plane as in figure 11 where the solar ecliptic longitude angle $\emptyset$ is the abscissa and latitude θ is the ordinate. The center of a region in each latitude range was chosen to correspond to average spiral angles of $\emptyset = 135°$ and $\emptyset = 315°$.

The numbers in the intervals in figure 11 represent the total number of individual 4.8 second interplanetary measurements occurring during the first five orbits. It can be seen that the numbers range from a high of 385 near the average spiral angle pointing toward the sun to a low of zero in a direction approximately opposite to this. The grouping of high values near the spiral angle pointing toward the sun mark this very definitely as a negative sector (negative defined as toward the sun; positive defined as away).

Upon examing the distributions for each orbit, it was generally a simple matter to ascertain whether the orbit belonged to a positive or negative sector. Consecutive orbits of the same polarity were then collected forming eight groups (four recurring sectors) during the two solar rotations from October 4 - November 27. Summary distributions similar to figure 11 were constructed for all eight sectors and from these plots, contours of equal occurrence were drawn. These are illustrated in figure 12 where the value one designates that expected for isotropic distribution, three designates three times an isotropic distribution, etc. Vertical lines at $\emptyset = 135°$ and 315° represent theoretical spiral angles for a 440 km/sec solar wind. There is a clear tendency for fields to group themselves

near the spiral angle pointing either toward or away from the sun. In all cases the 0.1 dotted contour indicates a paucity of fields in the direction opposite to the maximum. The preference for fields to be near the ecliptic plane is also apparent from figure 12 although a substantial number of fields point appreciably out of the ecliptic. During the fifth sector there is a filament of positive polarity occurring during the predominantly negative sector. The fields forming this filament near $\emptyset = 120^{o}$ in Sector 5 occur during the interval 0140-0430 on orbit 22 and have been presented in figure 4. The angular change of $\emptyset$ occurring near 0430 takes place over a time interval of 10 minutes.

The recurrence properties of the IMP-2 sectors can be investigated with the aid of figure 13 where the sector polarity has been superposed on 27 day K_p diagrams. Shown at the top of the figure are the average IMP-1 recurring sectors for solar rotations 1784-1786, and at the bottom the Mariner 4 data and K_p. The recurrence of the four IMP-2 sectors during the second solar rotation is quite clear with the boundaries reappearing within a day or two of their position on the previous solar rotation. In addition, the correspondence to the IMP-1 sectors observed one year earlier is quite good. Not only are four sectors present as at the time of IMP-1 but their positions are approximately the same. The size of the four sectors have changed slightly during the interval between IMP-1 and the IMP-2 observations.

Agreement between the IMP-2 sectors and the Mariner 4 sectors immediately following IMP-2 is not as good. Mariner 4 early in its flight was ahead of the earth in its motion around the sun and later passed behind the earth at a distant of about 3000 R_E. Sector boundaries would then be expected to arrive at the earth before arriving at Mariner 4 but the

correction is always less than a day in the data shown, (Davis, 1965). There is a general correspondence between IMP-2 and the first solar rotation of Mariner 4 but the sectors begin to evolve quite rapidly during subsequent rotations. As pointed out by Coleman et. al., (1966), May through November 1964 represented a period of minimum solar activity where stable sector patterns might be expected to occur. The evolution of the patterns in early 1965 may be related to increasing solar activity.

The IMP-1 result showing that geomagnetic activity reaches a peak about 2/7 of the way through a sector has been studied with the IMP-2 results. General agreement with this result can be deduced from figure 13 but a more refined analysis such as was used on IMP-1 (Wilcox and Ness, 1965) better demonstrates the agreement and is shown in figure 14. To prepare this figure the daily sum of Kp was assigned to each day and the duration of each sector was normalized to a value of one. The ordinate in figure 14 represents the average daily sum at the position within the sector given by the abscissa. The four positive and four negative sectors were treated separately and are represented by plus and minus signs in figure 14. The agreement between figure 14 and the IMP-1 results is very good with the peak in each case occurring early in the sector and a minimum at the end. The values of Σ Kp are also in good agreement at the peaks and at the minima. The three high positive values near the end of the sector can be traced to high Kp values occurring after the passage of a sector boundary. These high Kp's raise the Kp daily sum for the period at the end of a sector which was actually quiet. Comparing the Mariner 4 sectors and Kp in figure 13, it appears as if high Kp values occur near the end of a sector. Consideration of the earth-Mariner position relationship mentioned above would tend to shift the sector crossings such that the high Kp's would

occur early in the sector but it is not clear that the correction would be large enough to bring the results into agreement with the IMP-1 and IMP-2 results.

The distribution of field magnitude within a sector shows a tendency for higher fields to occur early in a sector such as was observed on IMP-1, but frequent passage through the magnetosphere precludes an analysis similar to that carried out on IMP -1 data.

To investigate the relation of sector structure to field in the magnetosheath, an analysis was performed identical to that used for the interplanetary field. The distribution of fields in the 96 regions was obtained for each sector and contours were again drawn. The distribution was found to be highly anisotropic in a manner similar to the interplanetary fields. From the contour plots an average $\emptyset$ angle was estimated for both interplanetary and magnetosheath fields for each sector. In figure 15 the average field magnitudes are plotted at the corresponding $\emptyset$ angles at positions corresponding to the average shock positions in the solar ecliptic plane. Positive sector interplanetary fields are represented by the solid vectors at the inner shock wave and corresponding magnetosheath fields are represented by dashed vectors. Negative sector results are shown at the outer shock wave (which has been duplicated for clarity). The average θ's for each sector are always less than 16^{o}.

In figure 15 it can be seen that average magnetosheath fields point generally towards dusk and dawn for positive and negative sectors respectively. It is clear that the smaller interplanetary fields should experience an angle change at the shock in order that the normal field component be continuous across the shock, but the angle change in figure

15 appears to be larger than expected from this argument. The reason for this is that the vectors in figure 15 were derived from data taken throughout the magnetosheath and therefore represent not only the effect of the shock wave but the effects of interaction with the magnetosphere. The directions of the average magnetosheath field suggest that the fields tend to align themselves tangent to the magnetosphere after undergoing an initial angle change at the shock.

SECTION 6. THE MAGNETOSPHERE

When IMP-2 is in the magnetosphere on the sunward side of the earth the fluxgate sensors are usually saturated and accurate measurements are seldom possible. As the orbit moves toward the dawn meridian in solar ecliptic coordinates, the field strengths in the outer magnetosphere decrease below the saturation level and measurements are obtained. As time progresses an increasing fraction of each orbit is spent within the magnetosphere and after orbit 77 the spacecraft is always completely within the magnetosphere. IMP-2 is therefore able to perform an extensive mapping of the dawn-to-midnight region of the magnetosphere between approximately 9 to 16 R_E.

One of the most striking characteristics of magnetic field data in this dawn-to-midnight region is the absence of large fluctuations of the field in the frequency range of cycles per second. Values of Δ are typically 0.5γ in fields up to 40γ and values of 0.2γ or 0.3γ (characteristic of interplanetary space) often occur in the weaker magnetosphere fields. Quasi-sinusoidal fluctuations with periods of several minutes and amplitudes of several gammas are more common, particularly in the weaker fields near the equatorial plane.

Primary emphasis in this phase of IMP-2 magnetosphere analysis has been placed on studying the average magnetic field topology with special attention given to the formation of the tail in the dawn-to-midnight region. For this purpose hourly averages in solar magnetic coordinates were used. This coordinate system is equivalent to a geomagnetic local time and latitude coordinate system. It is the most convenient system to investigate the distortion of the approximately dipole field close to the earth where the dipole orientation is as important as the solar wind direction.

The projections of the field in the solar magnetic XY plane are plotted and shown in figure 16. The trajectory of IMP 2 is such that the spacecraft is always well below the solar magnetic equatorial plane on the outbound portion of each orbit but nearer the equatorial plane on the inbound portion of the orbit. Whether the spacecraft crosses the equatorial plane before the detectors saturate depends on the orientation of the dipole when the spacecraft is inbound in the region 10-12 R_E. Since the dipole axis makes an angle of 11.5° with the rotational axis, this orientation depends on universal time. Only for a limited range of dipole orientations does the spacecraft cross the equatorial plane and make measurements in the northern hemisphere.

Figure 16 shows the projection of more than 350 hours of data which represents approximately 50 percent of the available data. Data from below the equatorial plane near apogee in the midnight hemisphere has been eliminated to prevent crowding in this graphical presentation. The fact that almost all measurements are below the equatorial plane is noted readily since the fields generally point away from the earth. The fields that do not point away from the earth, near X = -9, Y = -4, are measurements from above the equatorial plane. A dipole field would have a radial projection at points off the equatorial plane so the non-radial nature of the fields in figure 16 illustrates how the field is swept back to begin the formation of the tail by the solar wind.

The measurements in figure 16 show good correspondence among themselves in the various XY positions in spite of the fact that the measurements were made as much as 7 R_E below the equatorial plane. This observation suggests that at least to a first approximation, an entire magnetic

field meridian plane is swept back towards the tail by the solar wind. These hypothetical distorted field planes are sketched with dashed lines in figure 16. The eight numbered curved meridian surfaces are shown in figures 17a and b where total field magnitudes have been plotted at the angle the field makes with the equatorial plane. The location of the foot of each vector is the solar magnetic Z position of the measurement and the XY position measured along the curved surfaces of figure 16. Undistorted dipole field lines are included in figure 17 for comparison. Solid vectors indicate that the sun was below the magnetic equatorial plane and dashed vectors indicate the sun was above this plane.

For surface 1 in figure 17 the observed field direction agrees well with the theoretical dipole field out to 12 R_E. Beyond this distance the field lines begin to be distorted so that they are somewhat more radial than a dipole. The position where dipole-like fields near the equatorial plane turn over and point toward the earth appears to lie above the equatorial plane when the geomagnetic latitude of the sub-solar point is negative. For surface 2 the radial distortion is more pronounced with the field lines being dragged out in a manner that is reminiscent of measurements near the midnight meridian (Ness, 1965; Cahill, 1967). Weaker fields are seen near the equatorial plane as reported by Speiser and Ness (1966).

Surfaces 3 and 4 have less data due to spacecraft shutoff during part of the time the satellite was within this region. Few measurements are made above the equatorial plane but two in section 4 suggests a distinctly radial field near 10 R_E. Surfaces 5 and 6 in figure 17b confirm this and show that the generally solar-antisolar fields characteristic

of the tail may extend into the magnetosphere as far as 9 R_E near the midnight meridian plane. Surface 5 provides further illustration of solar wind directional control of the position of the inner edge of the neutral sheet. When the solar wind is incident on the dipole at a positive solar geomagnetic latitude, three dashed vectors near the equatorial plane point toward the earth, demonstrating that the field reversal region now extends below the magnetic equatorial plane. When the sun is at southern geomagnetic latitudes the satellite must go further north before the field reverses and points toward the earth. The two large vectors above the equatorial plane beyond 12 R_E pointing away from the earth were taken about 16 hours after a sudden commencement storm on March 12 when the magnetic latitude of the sun was -14°. During the following hour the field reversed direction and the hourly average is the small vector above the equatorial plane in surface 4. This region of reversal was apparently moved 1.6 R_E above the equatorial plane and the field reached a minimum of 8γ at the time of the reversal.

The fields well below the equatorial plane in surface 6 point primarily in the antisolar direction, but also have a small southward component even when the solar wind is incident from southerly geomagnetic latitudes. This observation is confirmed in surfaces 7 and 8 although at the time of these later measurements the sun is more often above the solar magnetic equator.

VII SUMMARY

The IMP 2 satellite investigated magnetic fields in interplanetary space, the magnetosheath and the magnetosphere between October 4, 1964 and April 7, 1965. This was a time of generally low solar activity but several moderate magnetic storms occurred most of which were of the recurring type often said to be associated with M regions.

Over 325 hours of interplanetary data were obtained between October 4 and November 30 during solar rotations 1795 - 1797. IMP 2 detected the interplanetary field direction partitioned into four recurrent sectors similar to those sections seen by IMP 1 one year earlier. However, the sectors seen by the IMP 2 were of approximately equal size, so that small changes in the sizes of the sectors had occurred. The 4 sectors seen by IMP 2 on the first solar rotation reappeared in approximately 27 days. The positions and sense of sectors agreed reasonably well with IMP 1 measurements covering solar rotations 1783-1785.

The correspondence with Mariner 4 measurements made immediately after IMP 2 was not as clear. A relatively stable pattern of 27 day recurring magnetic activity was present between IMP 1 and IMP 2 intervals whereas this stable pattern began breaking up late in 1964. This suggests that evolving solar magnetic fields associated with the new susnspot cycle led to the changing sectors seen by Mariner 4 and the disagreement with IMP 2.

High interplanetary fields tended to occur early in the various sectors as they swept past the earth, but frequent and long perigee gaps

precluded an extensive analysis of the internal sector structure. High Kp values also showed a strong tendency to occur early in a sector with low Kp values occurring near the end of a sector. Both of these results are in good agreement with the IMP 1 results (Wilcox and Ness, 1965).

The direction of the interplanetary field in any one sector varied considerably in direction but tended to be distributed about the theoretical spiral angle. The direction was often quite constant for periods of hours at a time, however, at other times it changed gradually over durations ranging from a few minutes up to hours. On other occasions the field directions changed abruptly by as much as 180° between measurements taken 20.5 seconds apart. The few apparent sector boundaries seen by IMP 2 tended to correspond to less rapid angle changes. During each sector the ratio of the number of fields along the spiral angle in one direction to that in the opposite direction was typically 100:1.

The average interplanetary field direction for each sector was always near the solar ecliptic plane and the angle in the ecliptic plane was usually within 25° of the average theoretical spiral angle of 135° (315°). Magnetosheath fields during each sector were found to exhibit a highly anisotropic distribution with average fields pointed towards the dusk and dawn meridians for away and toward sectors respectively. This clear relation between the interplanetary field direction and the magnetosheath direction shows that interplanetary fields are convected through the earth's bow shock front where they are compressed and thus increase in magnitude while experiencing relatively small changes in direction. The average fields computed from measurements made throughout the magnetosheath tend to lie nearly parallel to the average

shock front so that the field component normal to the shock is less than the interplanetary field normal to the shock. Since the normal components across the shock must be continuous, this result suggests that the magnetosheath field direction is determined not only by the interplanetary field and its passage through the shock but is also strongly influenced by interaction with the magnetosphere. The apparent alignment of the average magnetosheath fields with the shock is more likely an alignment of the fields tangent to the magnetopause. This result indicates that the interplanetary field is draped around the magnetosphere as the solar wind flows around it.

Investigation of the IMP-2 magnetic field data on an expanded time scale has revealed apparently frequent motion of both the bow shock and the magnetopause. Multiple shock crossings were observed on the great majority of orbits and multiple magnetopause crossings on approximately half the orbits. Shock crossings typically occurred in less than one minute and often in less than the 20.5 seconds between measurements. Clear shock crossings could often be resolved when they were separated by only a few minutes in time but more typically they were tens of minutes apart. Magnetopause crossings generally took somewhat longer than one minute and were generally more difficult to resolve, particularly when the magnetosheath fields were aligned approximately parallel to magnetosphere fields and both fields were undergoing fluctuations. The time intervals between multiple magnetopause crossings were typically 10 to 20 minutes and usually not more than 5 or 7 crossings were observed on any one pass.

Since the satellite is in motion, it is impossible to convert boundary crossing times to distances without assuming a velocity for the boundary. With the available data from only one satellite it is also impossible to distinguish between traversals of the boundaries due to radial motion of the entire magnetopause or waves propagating on a relatively fixed boundary. The variability of boundary positions for all the orbits suggests that radial motion is important on long time scales but waves may also lead to the multiple crossings.

Comparisons of magnetic field boundary positions with those simultaneously determined from two plasma experiments on board IMP 2 were generally very good. Both the >5 ev electron current of the GSFC retarding potential plasma analyzer and the ion currents measured by the MIT Faraday cup experiment showed a marked enhancement in the magnetosheath relative to either the magnetosphere or interplanetary space. The agreement between GSFC magnetic field and MIT plasma shock positions was particularly good when comparisons were made on the finest time scale possible, that is 5-80 seconds depending upon relative position in the telemetry format of the shock crossing.

Identifications of the magnetopause by the three experiments were in good agreement on most passes but there were some interesting exceptions. On some occasions there was evidence for enhanced plasma detector currents inside the magnetopause as identified by the magnetic field measurements. This suggests direct entry of solar wind plasma into the magnetosphere which could serve as a source of trapped particle radiation. On several passes through the magnetopause there was an

absence of either a magnitude or angle discontinuity in the magnetic field data. This circumstance was invariably accompanied by a gradual change in plasma currents from high magnetosheath values to low magnetosphere values rather than the typical sharp discontinuity. Clearly one prerequisite to having this condition is that magnetic fields in the magnetosheath be aligned parallel to the magnetosphere fields in order not to have an angle discontinuity. Except for parallel fields, other circumstances necessary to produce this condition have not yet been discerned.

Often fields within the magnetosheath are relatively constant in direction and magnitude while at other times the fields exhibit important fluctuations with periods of fractions of a second to minutes. On occasion the magnetosheath fields rapidly change from very disturbed to very quiet conditions. No spatial variations are readily apparent other than a tendency of the more quiet fields to occur further from the subsolar point. The character of the magnetosheath field must be dependent on interplanetary conditions which may change the nature of the interaction at or inside the shock.

Magnetic field fluctuations in the magnetosphere are particularly evident near the subsolar point in the region where trapped and quasi-trapped particles are found. Nearer the dawn meridian fluctuations with periods of seconds are of decreasing importance and most of the energy is associated with fluctuations with periods of minutes. The regions of the magnetic tail in the midnight hemisphere are often devoid of any fluctuations, particularly away from the solar magnetic equator. Nearer the solar magnetic equator waves with periods of minutes are often apparent.

The average topology of the geomagnetic field has been studied by plotting hourly average vectors in the solar magnetic equatoral plane and in curved meridian surfaces perpendicular to this equatorial plane. The equatorial plot illustrates how the goemagnetic field is swept back towards the tail by the solar wind. This effect is apparent even quite close to the subsolar point. Meridian surface plots demonstrate how the field lines begin deviating from almost dipole lines near the dawn meridian in a manner which gradually increases until the fields are directed primarily in the solar or anti-solar direction in the northern or southern hemisphere near midnight. The fields are found to be directed predominantly parallel to the solar magnetic equatorial plane and in a radial direction near the midnight meridian as close to the earth as 9 R_E. The small radius of curvature for field lines crossing the equatorial plane at these distances seems certain to be a limiting factor in the trapping of particles in durable 360^o longitude drift orbits.

The effect of the solar wind direction in controlling the position of the inner edge of the neutral sheet has also been studied with the IMP 2 measurements. Far from the earth the solar wind direction controls the average position of the neutral sheet (Speiser and Ness 1966) whereas near the earth, the geomagnetic dipole predominates and field lines have a raidal component away from the earth above the magnetic equatorial plane. IMP 2 measurements clearly show that when the sun is at a southernly magnetic latitude, the solar wind forces this region of radial component reversal above the solar magnetic equator whereas

when the sun is at a positive magnetic latitude the reverse is true. There appears to be a smooth transition from complete control of the radial field component reversal by the solar wind far from the earth to complete control by the dipole near the earth. During one pass in a storm the region of reversal was particularly clear at a position 1.6 R_E above the solar magnetic equatorial plane at a radial distance of 12 R_E when the sun was 14^o below the magnetic equator.

ACKNOWLEDGEMENTS

We are indebted to our colleagues Mr. C. S. Scearce and Mr. J. B. Seek who carried out the instrumentation and testing of the IMP 2 Magnetic field experiment. We appreciate the use of the plasma data of Mr. G. P. Serbu of GSFC and gratefully acknowledge fruitful discussions and data comparisons with Dr. Joseph Binsack of MIT.

REFERENCES

Anderson, K. A. Energetic Electron Spikes In and Beyond the Transition Region, Proc. Int. Conf. on Cosmic Rays, London, Vol. 1 520-527, 1965.

Balasubrahmanyan, V. K., D. E. Hagge, G. H. Ludwig, and F. B. McDonald, Galactic Cosmic Rays at Solar Minimum, 1965, Proc. Int. Conf. on Cosmic Rays, London, Vol. 1, 472-436, 1965.

Binsack, J. H., Private Communication. See also MIT PhD Thesis 1966.

Bridge, H., A. Egidi, A. Lazarus, E. Lyon and L. Jacobson, Preliminary Results of Plasma Measurements on IMP-A. Space Research V, North Hollard Publ. Co. (1965) presented at COSPAR Florence, Italy, May 1964.

Davis, L., Jr., Private Communication

Davis, L. Jr., E. J. Smith, P. J. Coleman, Jr., and C. P. Sonett, Interplanetary Magnetic Measurements in The Solar Wind Edited by Robert J. Mackin and Marcia Neugebauer, Pergamon Press, New York 35-52, 1965.

Cahill, L. J., and P. G. Amazeen, The Boundary of the Geomagnetic Field, J. Geophys, Res., 68, 1835-1843, 1963.

Cahill, L. J., Jr., Inflation of the Magnetosphere Near 8 Earth Radii in the Dark Hemisphere, Space Research VI, North Hollard Publishing Co. (1967), presented at COSPAR, Buenos Aires, May, 1965.

Coleman, P. J., Leverett Davis, Jr., E. J. Smith, and D. E. Jones, Variations in the Polarity Distribution of the Interplanetary Magnetic Field, J. Geophys. Res. 71, 2831-2839, 1966.

Finch, H. F., and B. R. Leaton, the Earth's Main Magnetic Field, Epoch 1966.0, Monthly Notices, Roy. Astron. Soc. (Geophysical Supplement), 7, 314-317, November 1957.

Freeman, John W., Jr., The Morphology of the Electron Distribution in the Outer Radiation Zone and Near the Magnetospheric Boundary as Observed by Explorer 12, J. Geophys. Res. 69, 1691-1723, 1964.

Heppner, J. P. Recent Measurements of the Magnetic Field in the Outer Magnetosphere and Boundary Regions, GSFC preprint X-612-65-490, 1965.

Holzer, Robert E., Malcolm G. McLeod, and Edward J. Smith, Preliminary results From the OGO-1 Search Coil Magnetometer: Boundary Positions and Magnetic Noise Spectre, J. Geophys, Res, 71, 1481-1486, 1966.

Lincoln, J. Virginia, Geomagnetic and Solar Data, J. Geophys, Res., 70, 4963-4964, 1965.

Ness, N. F., The Earth's Magnetic Tail, J. Geophys, Res. 70, 2989-3005, 1965.

Ness, N. F., Observations of the Solar Wind Interaction with the Geomagnetic Field: Conditions Quiet, to be published in Proceedings of Belgrade Solar Terrestrial Relationships Interunion meeting, 1966.

Ness, N. F., C. S. Scearce and J. B. Seek, Initial Results of the IMP 1 Magnetic Field Experiment J. Geophys. Res., 69, 3531-3569, 1964.

Ness, N. F., and J. M. Wilcox, Solar Origin of the Interplanetary Magnetic Field, Phys. Rev. letters, 13, 461-464, 1964.

Ness, N. F. and John M. Wilcox, Sector Structure of the Quiet Interplanetary Magnetic Field, Science, 148, 1592-1594, 1965.

Patel, V. L. and A. J. Dessler, Geomagnetic Activity and Size of Magnetospheric Cavity, J. Geophys. Res., 71, 1940-1942, 1966.

Serbu, G. P. and E.J.R. Maier, Low Energy Electrons Measured on IMP 2, J. Geophys, Res., 71, 375 -3766, 1966

Speiser, T. W. and N.F. Ness, The Neutral Sheet in the Geomagnetic Tail: Its Motion, Equivalent Currents, and Field Line Reconnection Through It, J. Geophys, Res., January 1967.

Wilcox, John M. and N.F. Ness, Quasi-Stationary Corotating Structure in the Interplanetary Medium, J. Geophys, Res., 70, 5793-5805, 1965.

Wolfe, J. W., R. W. Silva and M. Myers, Preliminary Results for the Ames Research Center Plasma Probe Observations of the Solar-wind Geomagnetic Field Interaction Region on IMP-2 and OGO-1, Space Research VI, to appear, 1966.

FIGURE CAPTIONS

FIGURE 1 Projection of the IMP 2 orbit on the solar ecliptic plane at various times throughout the satellite lifetime. Three intervals are shown when a favorable spin axis-sun angle permitted continuous operation of the spacecraft.

FIGURE 2 Representative spin modulated raw data curves and best fit sinusoids determined by least squares procedures.

FIGURE 3 IMP 2 Orbit 4 magnetic field and plasma current data ($I_{negative}$) on October 8 - 9, 1964 illustrating observations of the magnetosphere, the magnetopause, the magnetosheath and interplanetary space. The high field region beyond 15 R_E between 0030-0130 probably represents the magnetosheath and thus motion outward of the bow shock wave.

FIGURE 4 IMP 2 Orbit 22 magnetic field and plasma current data on November 3-4, 1964. Clearly evident is the multiple crossing of the bow shock wave while the satellite was near apogee and thus almost stationary.

FIGURE 5 Individual magnetic field magnitude measurements and RMS deviations at 20.5 second intervals illustrating motion of the shock. This is an expanded data and time scale presentation of the multiple shock crossings shown in Figure 4.

FIGURE 6 Individual 20.5 second magnetic field vector measurements and theoretical fields in solar magnetic coordinates illustrating motion of the magnetopause as observed by IMP 2.

FIGURE 7 IMP 2 orbit 19 magnetic field data on October 30-31, 1964 illustrating clear and well defined magnetopause and shock crossings.

FIGURE 8 IMP 2 orbit 8 magnetic field and plasma current data on October 14-15, 1964 illustrating a diffuse or poorly defined magnetopause between 1200-1500 on the outbound orbit.

FIGURE 9 Presentation of the IMP 2 trajectory in the ecliptic plane for intervals when the spacecraft is within the magnetosheath. Satellite positions have been converted to the solar ecliptic XY plane by rotation in a meridian plane. Average magnetopause and shock positions have been sketched in with a dashed line. The innermost observation of the magnetopause occurred at 8.9 R_E and the outermost observation within 45° of the earth sun line was at 14.0 R_E.

FIGURE 10 IMP 2 interplanetary magnetic field magnitude distribution.

FIGURE 11 Sample of the subdivision into 96 equal solid angle portions of the solar ecliptic sphere as shown projected on a plane. Values indicate number of interplanetary field measurements occurring within each interval during the first sector observed by IMP 2.

FIGURE 12 Contours of equal field occurrence probability for 8 IMP 2 interplanetary sectors. Data has been normalized so that 1 designates isotropic distribution. Vertical dashed lines indicate theoretical spiral angles of 135° and 315°.

FIGURE 13 Kp diagrams with IMP 2 and Mariner 4 sectors superposed. Average IMP 1 sectors are included at the top of the figure.

FIGURE 14 Distribution of geomagnetic activity within a sector.

FIGURE 15 Average interplanetary and magnetosheath field magnitude plotted at the average $\emptyset$ angle for each of the IMP 2 sectors. Average solar ecliptic θ angles are all less than 16°.

FIGURE 16 Projection of hourly average magnetosphere fields on the solar magnetic equatorial plane. Dashed lines indicate the intersection of hypothetical meridian surfaces which approximately contain distorted dipole field lines.

FIGURE 17 The curved meridian planes are shown whose intersections with the solar magnetic equatorial plane were defined in figure 16. The hourly average magnetic field magnitude is plotted at the angle the field makes with the solar magnetic equatorial plane.

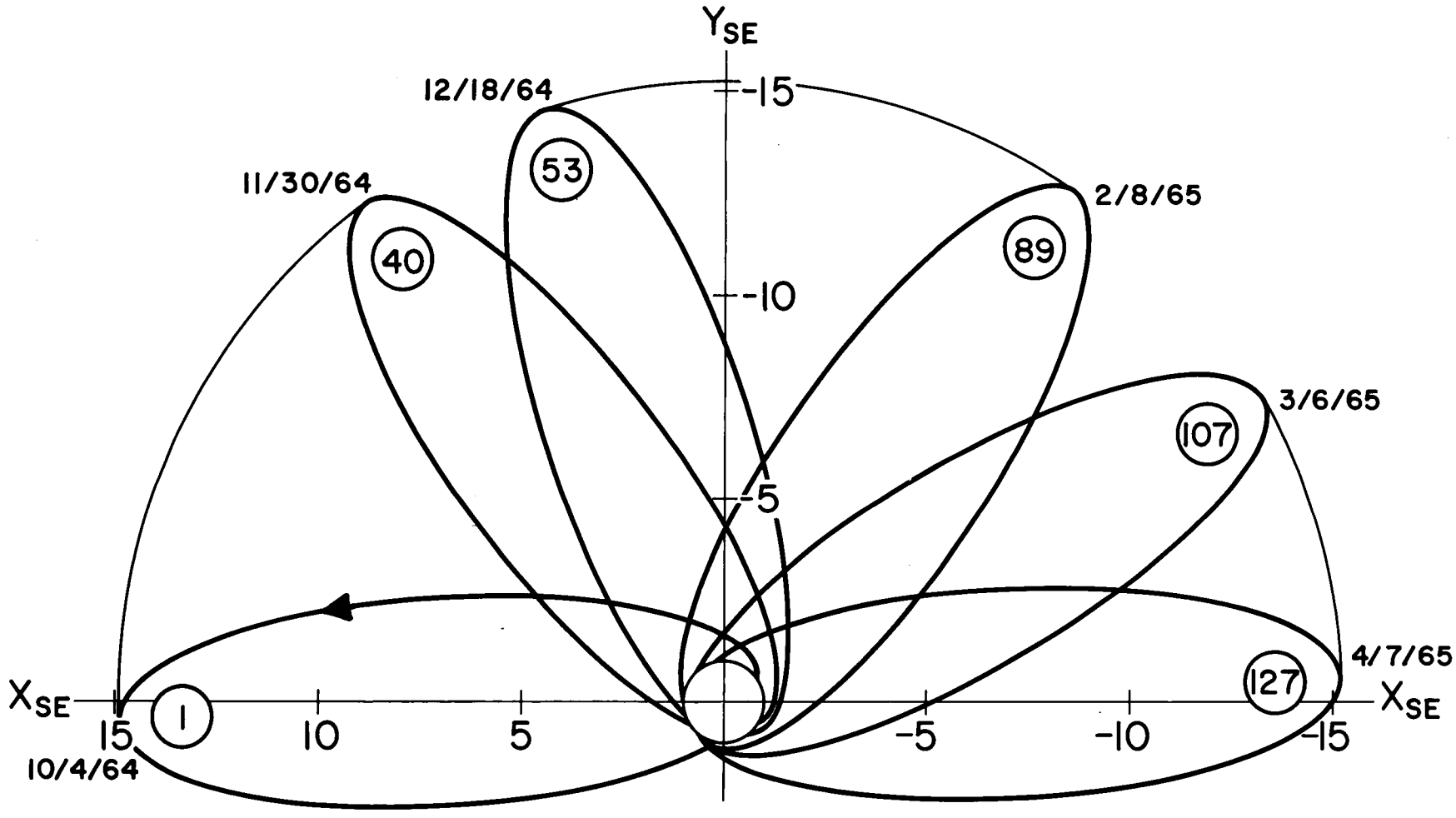

IMP-2 TRAJECTORY - SOLAR ECLIPTIC EQUATORIAL PLANE

FIGURE 1

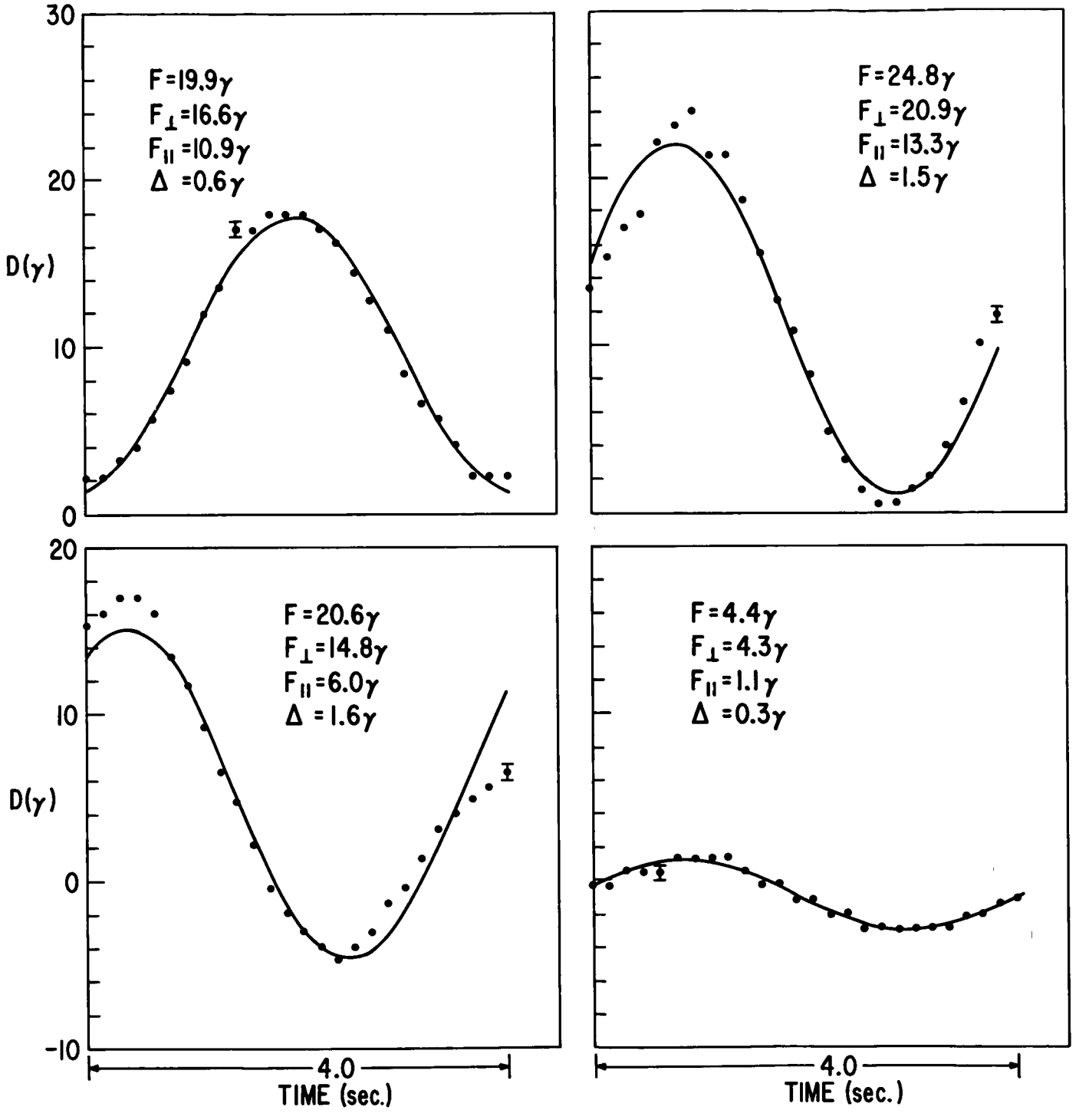

IMP-2 BEST FIT TO RAW DATA BY LEAST SQUARED ERROR

FIGURE 2

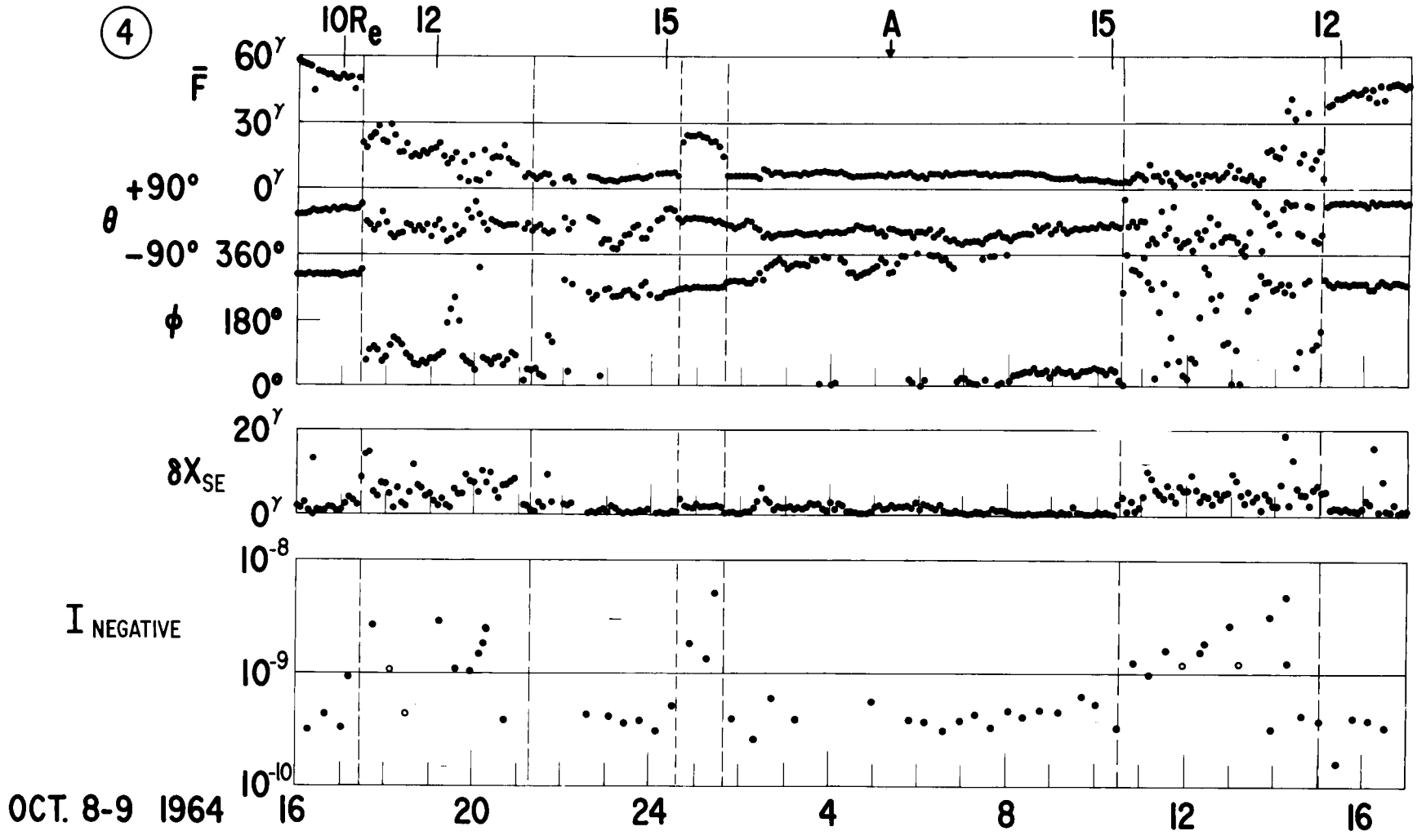
4
10Re
12
15
A
15
12
F
60γ
30γ
0γ
θ
+90°
-90°
360°
φ
180°
0°
δXSE
20γ
0γ
I NEGATIVE
10-8
10-9
10-10
OCT. 8-9 1964
16
20
24
4
8
12
16

FIGURE 3

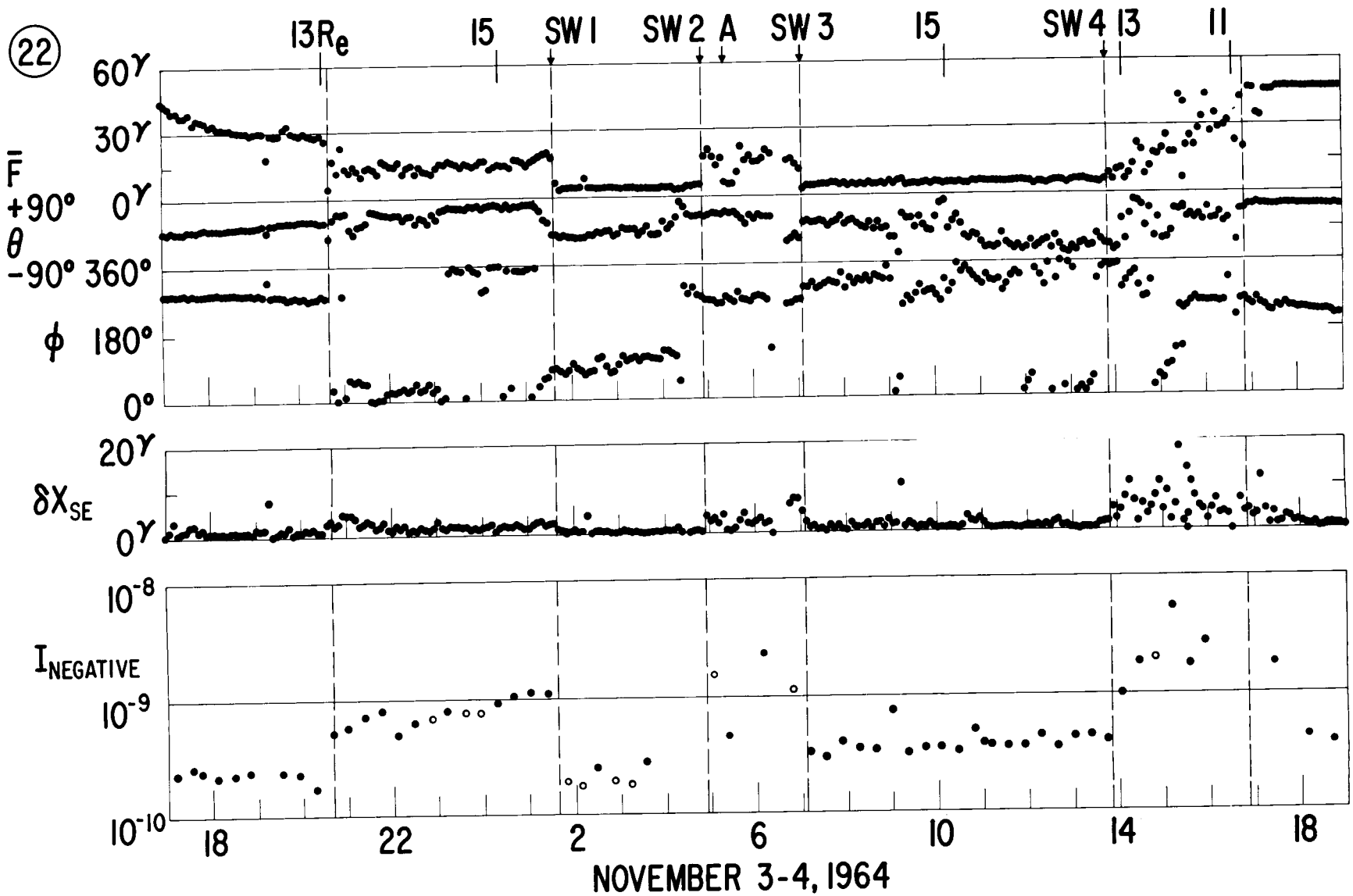
22
13Re
15
SW1
SW2
A
SW3
15
SW4
13
11
60γ
30γ
F̄
+90°
0γ
θ
-90°
360°
φ
180°
0°
20γ
δX_SE
0γ
10^-8
I_NEGATIVE
10^-9
10^-10
18
22
2
6
10
14
18
NOVEMBER 3-4, 1964

FIGURE 4

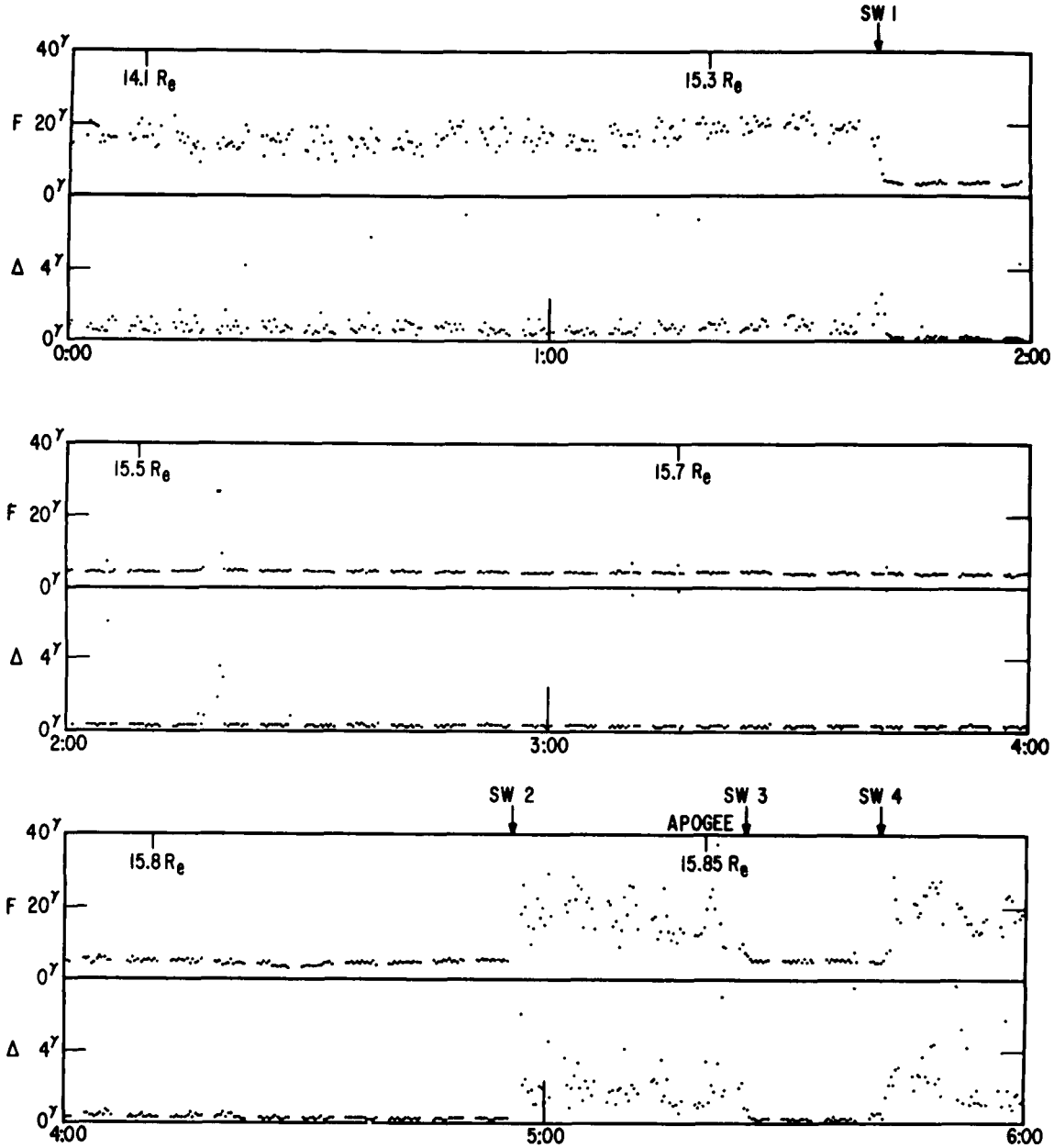

IMP-2 SHOCK MOTION ORBIT 22 NOVEMBER 3, 1964

FIGURE 5

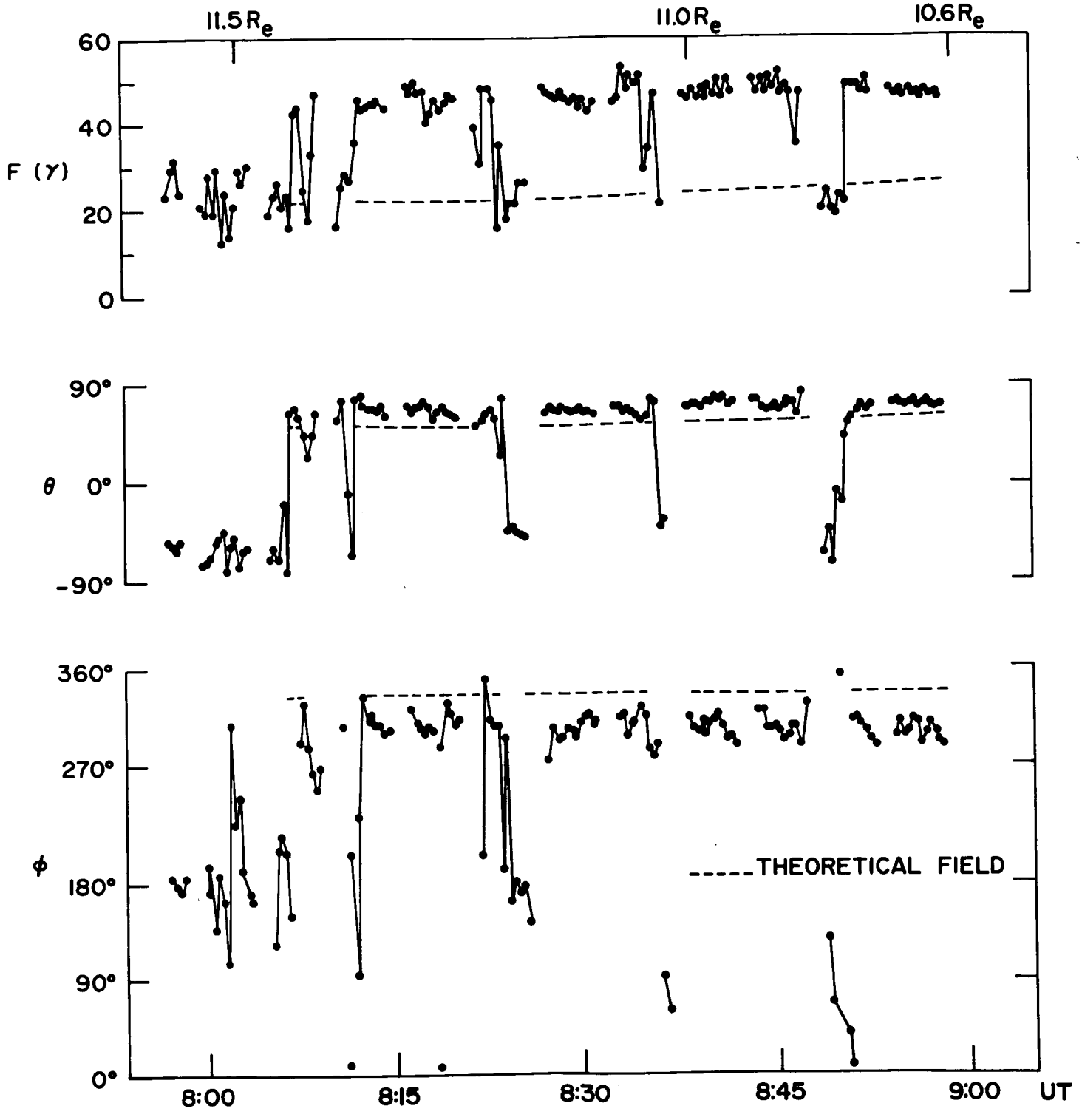

IMP II MAGNETOPAUSE MOTION ORBIT 28 INBOUND NOVEMBER 13, 1964

FIGURE 6

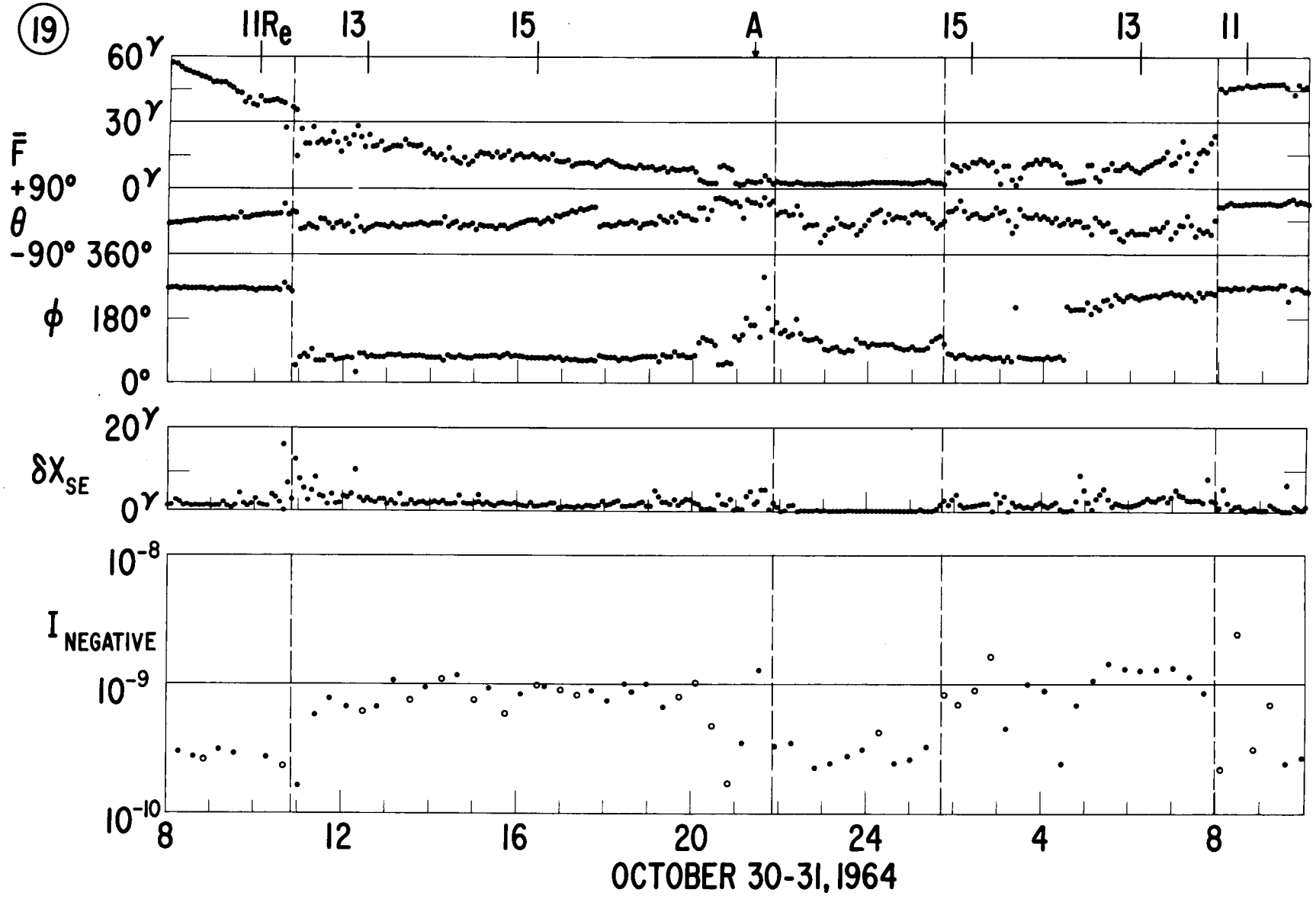
(19)
11Re
13
15
A
15
13
11
60γ
30γ
0γ
F̄
+90°
θ
-90°
360°
φ
180°
0°
20γ
δX_SE
0γ
10^-8
I NEGATIVE
10^-9
10^-10
8
12
16
20
24
4
8
OCTOBER 30-31, 1964

FIGURE 7

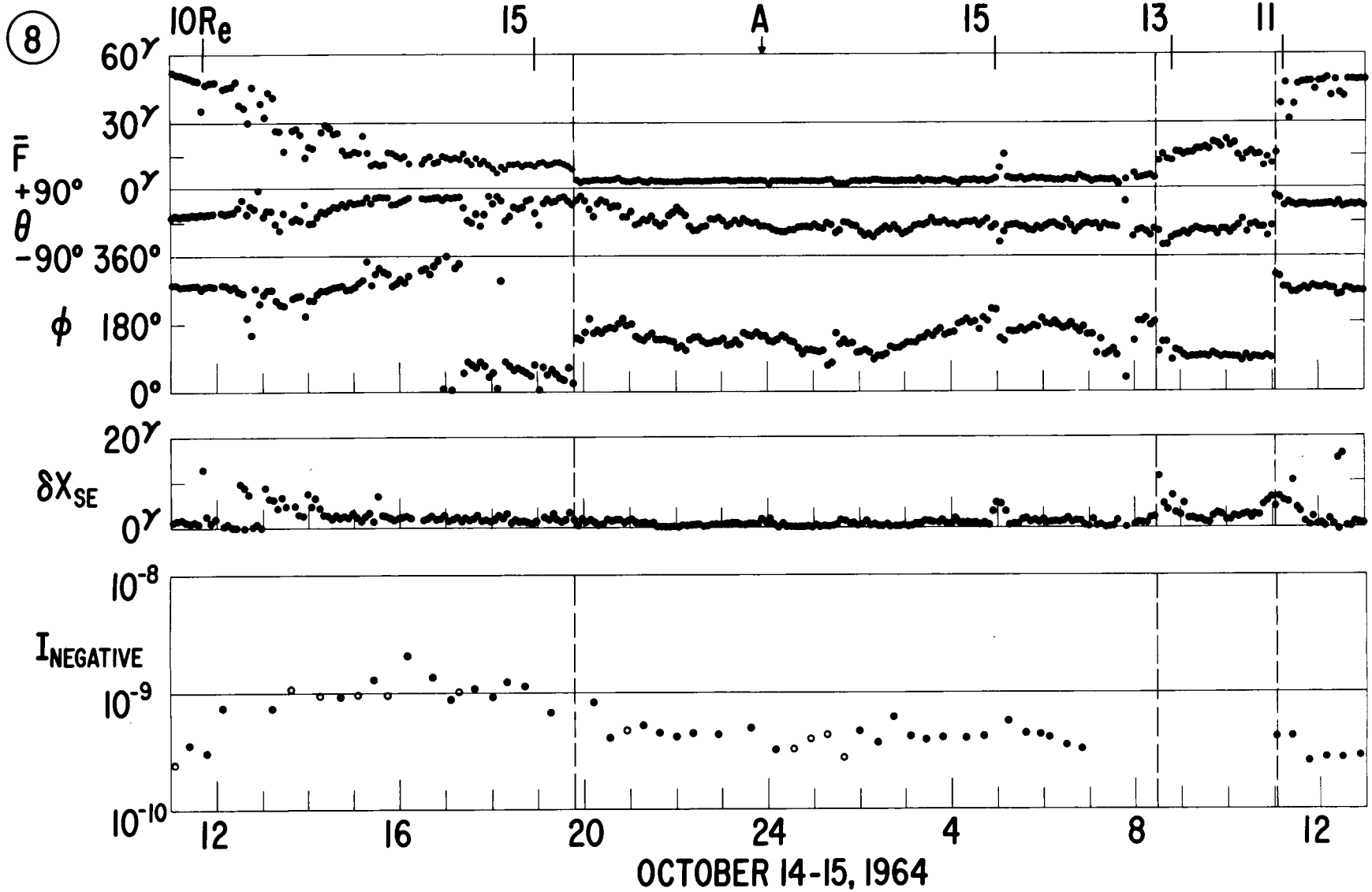
8
10Re
15
A
15
13
11
60γ
30γ
F̄
+90°
0γ
θ
-90°
360°
φ
180°
0°
20γ
δX_SE
0γ
10^-8
I_NEGATIVE
10^-9
10^-10
12
16
20
24
4
8
12
OCTOBER 14-15, 1964

FIGURE 8

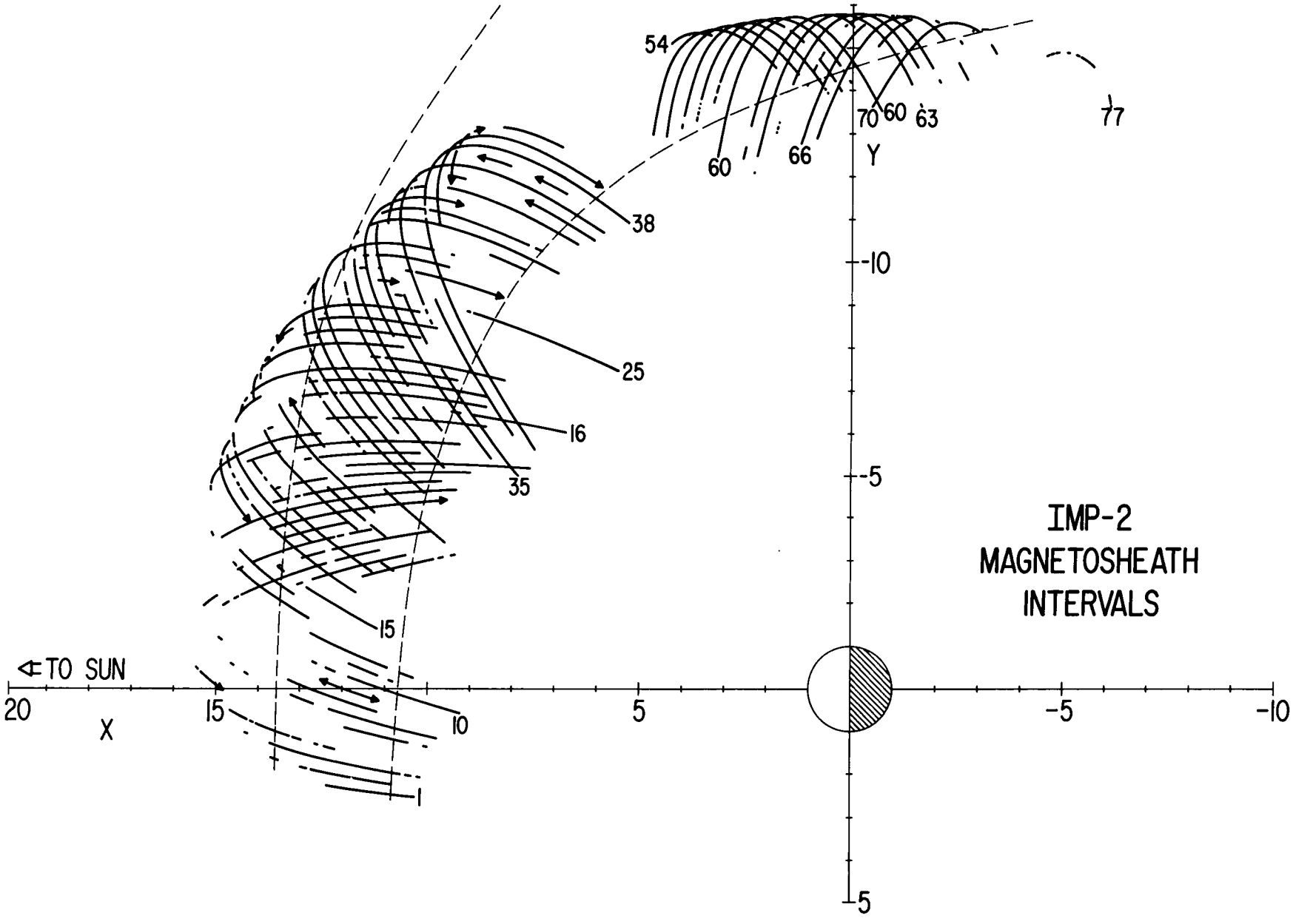
54
70
60
63
77
60
66
Y
38
-10
25
16
35
-5
IMP-2
MAGNETOSHEATH
INTERVALS
TO SUN
20
X
15
10
5
-5
-10
15
1
5

FIGURE 9

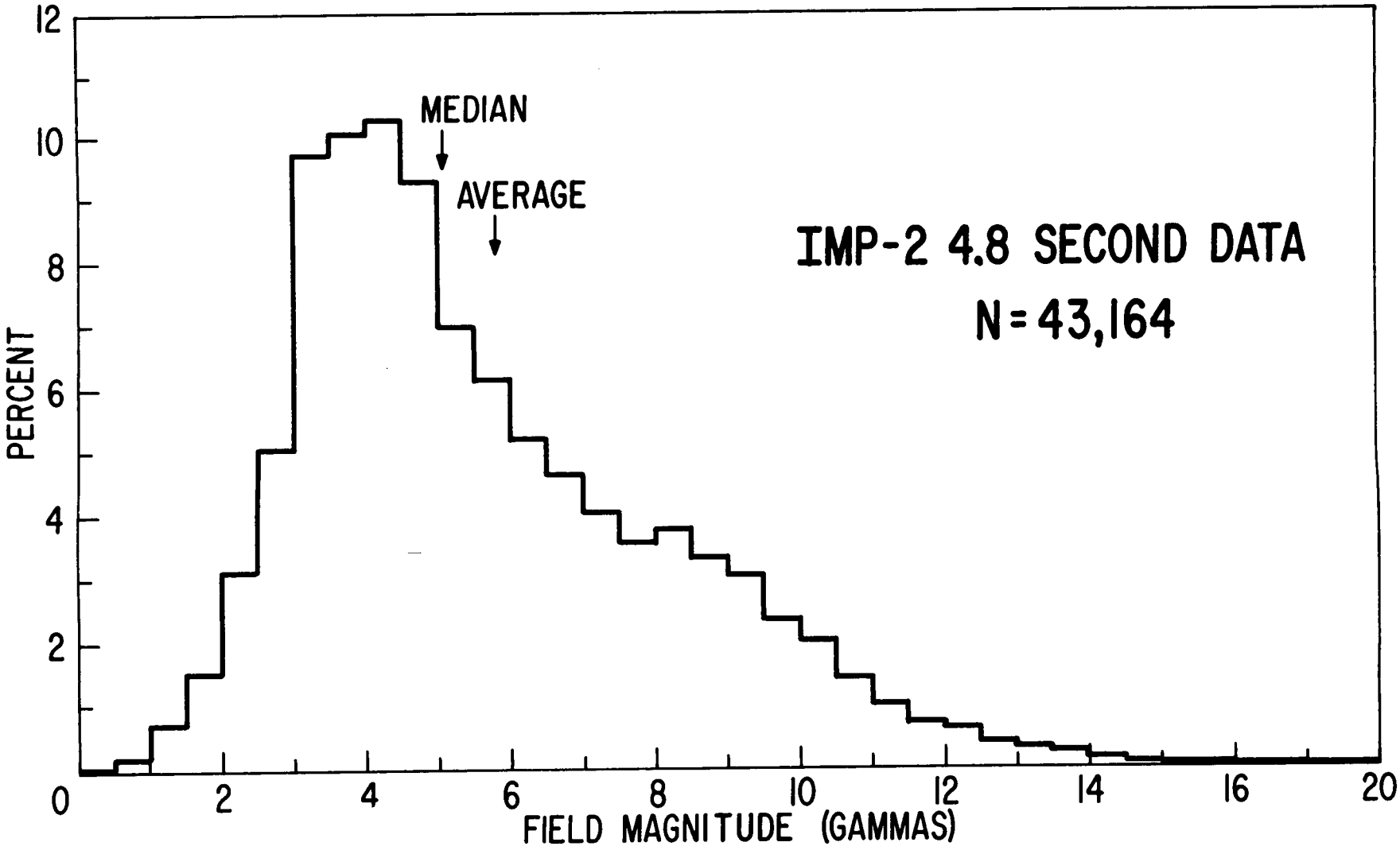
MEDIAN
AVERAGE
IMP-2 4.8 SECOND DATA
N=43,164
PERCENT
FIELD MAGNITUDE (GAMMAS)
0
2
4
6
8
10
12
14
16
20

FIGURE 10

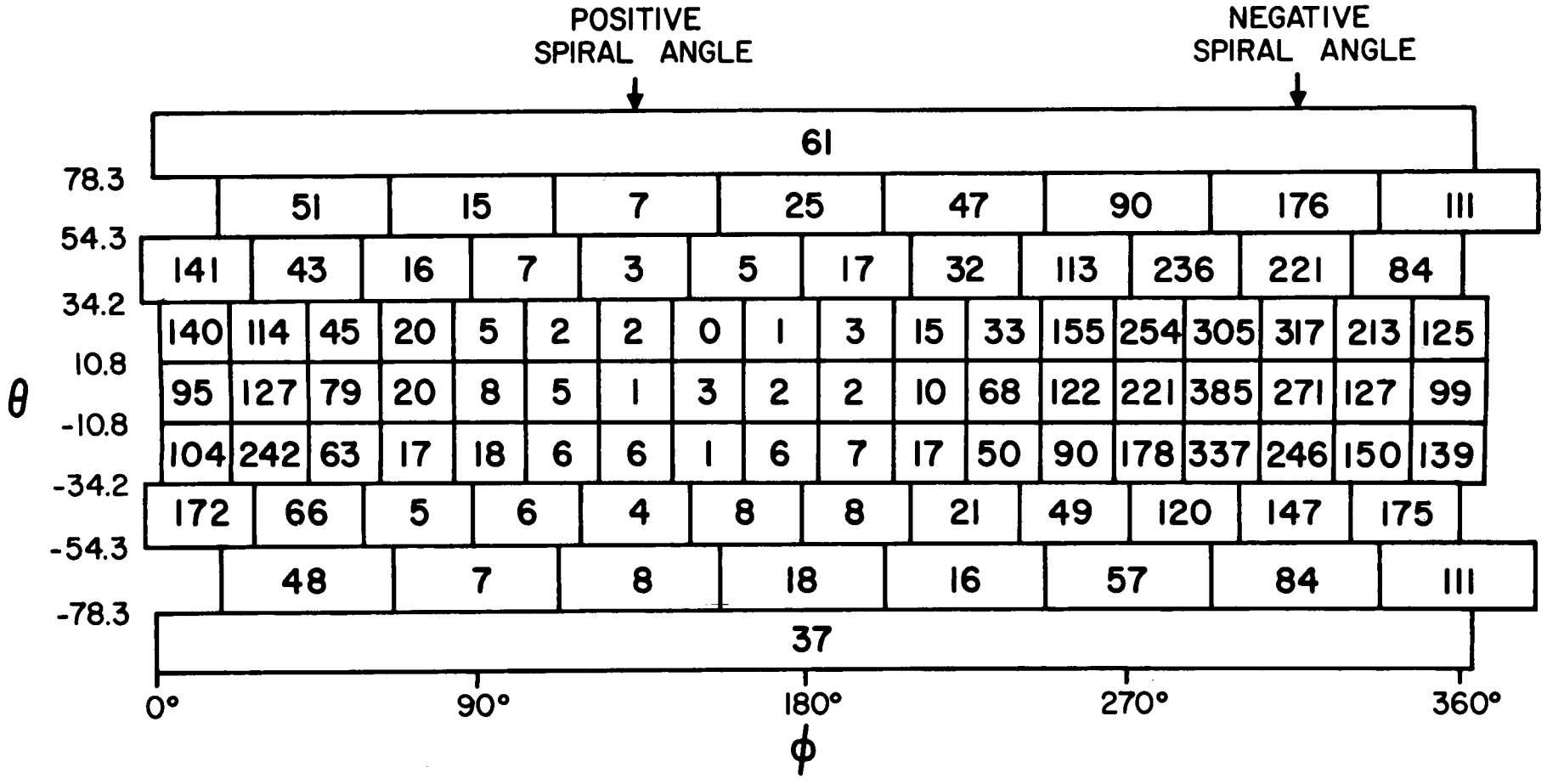

MAGNETIC FIELD SECTOR DIRECTIONAL DISTRIBUTION

FIGURE 11

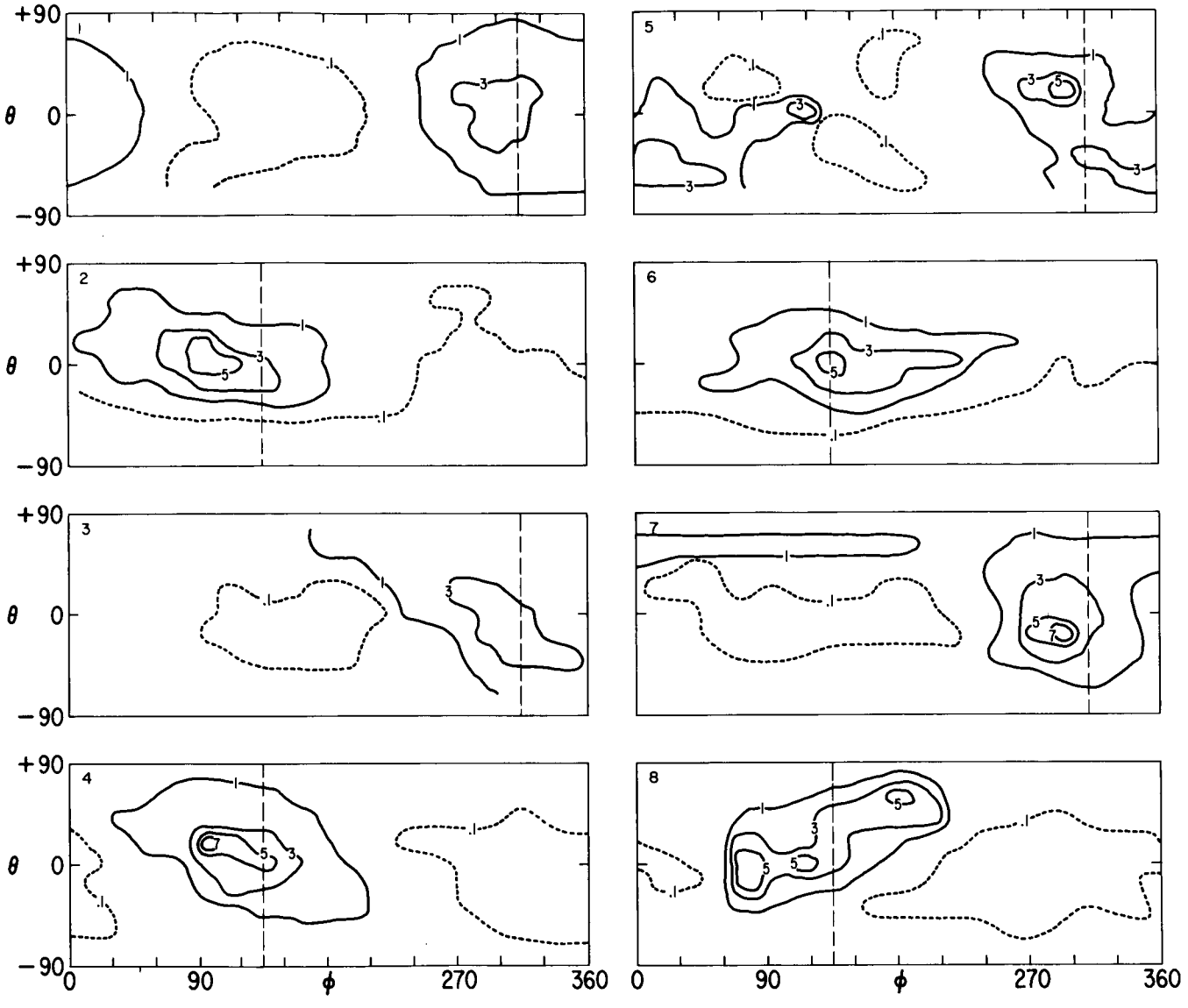

IMP-2 SECTORS OCT. 4, 1964 - NOV. 27, 1964

FIGURE 12

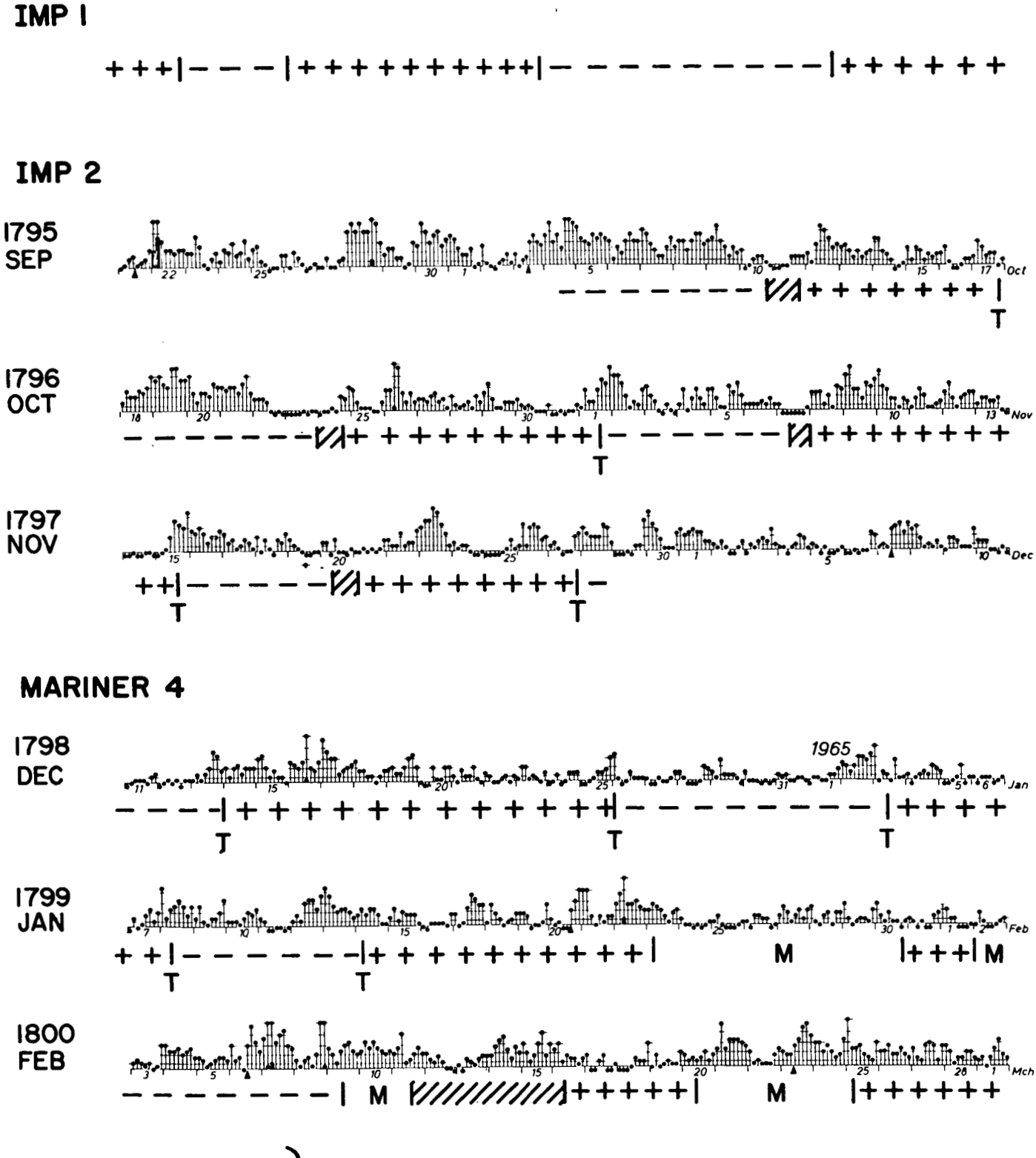
IMP 1
IMP 2
1795 SEP
1796 OCT
1797 NOV
MARINER 4
1798 DEC
1799 JAN
1800 FEB
1965
T
M
+ POSITIVE
− NEGATIVE
M MIXED
/// NO DATA
POLARITY OF INTERPLANETARY MAGNETIC FIELD

FIGURE 13

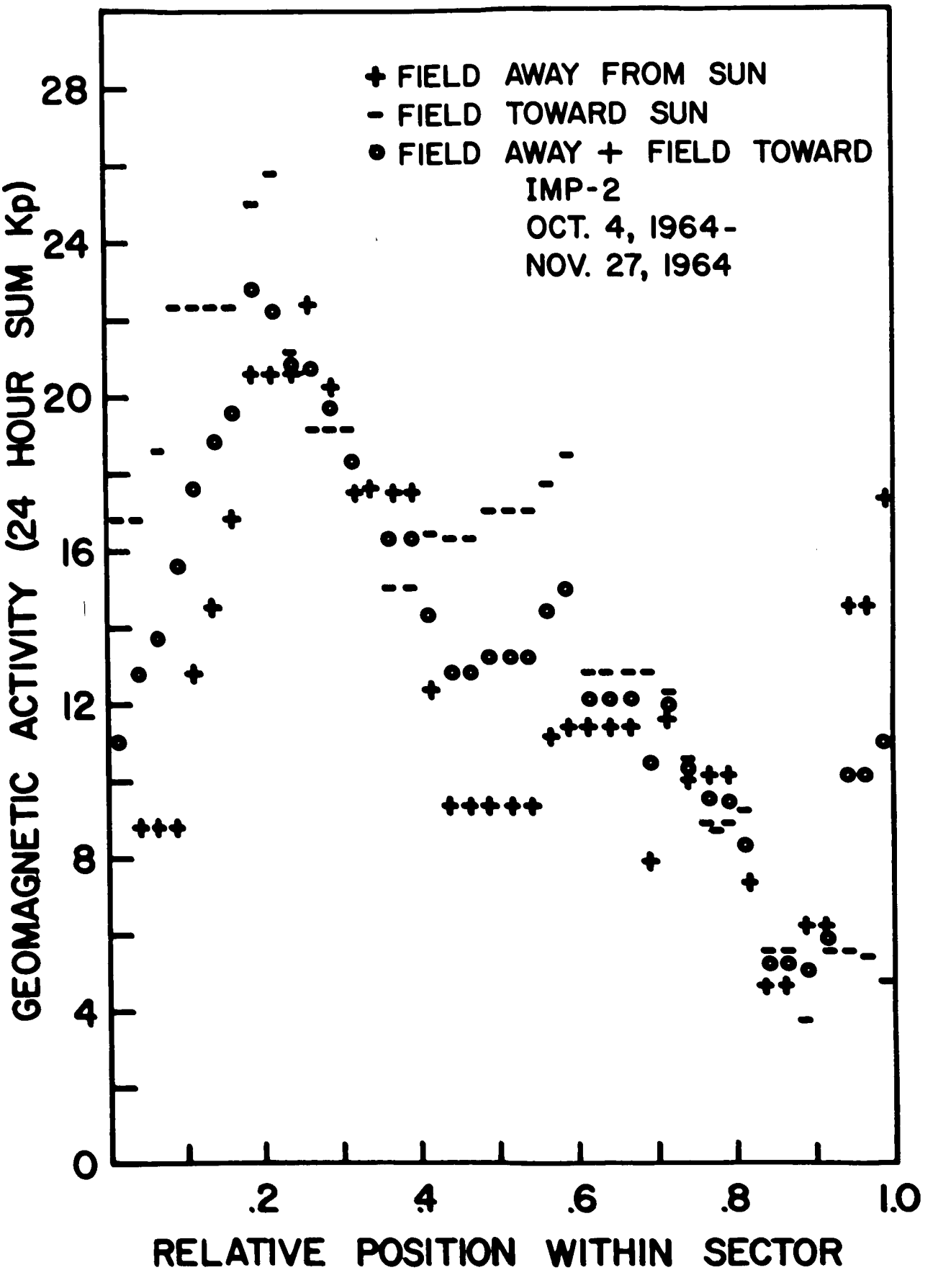
+ FIELD AWAY FROM SUN
- FIELD TOWARD SUN
• FIELD AWAY + FIELD TOWARD
IMP-2
OCT. 4, 1964-
NOV. 27, 1964
GEOMAGNETIC ACTIVITY (24 HOUR SUM Kp)
0
4
8
12
16
20
24
28
.2
.4
.6
.8
1.0
RELATIVE POSITION WITHIN SECTOR

FIGURE 14

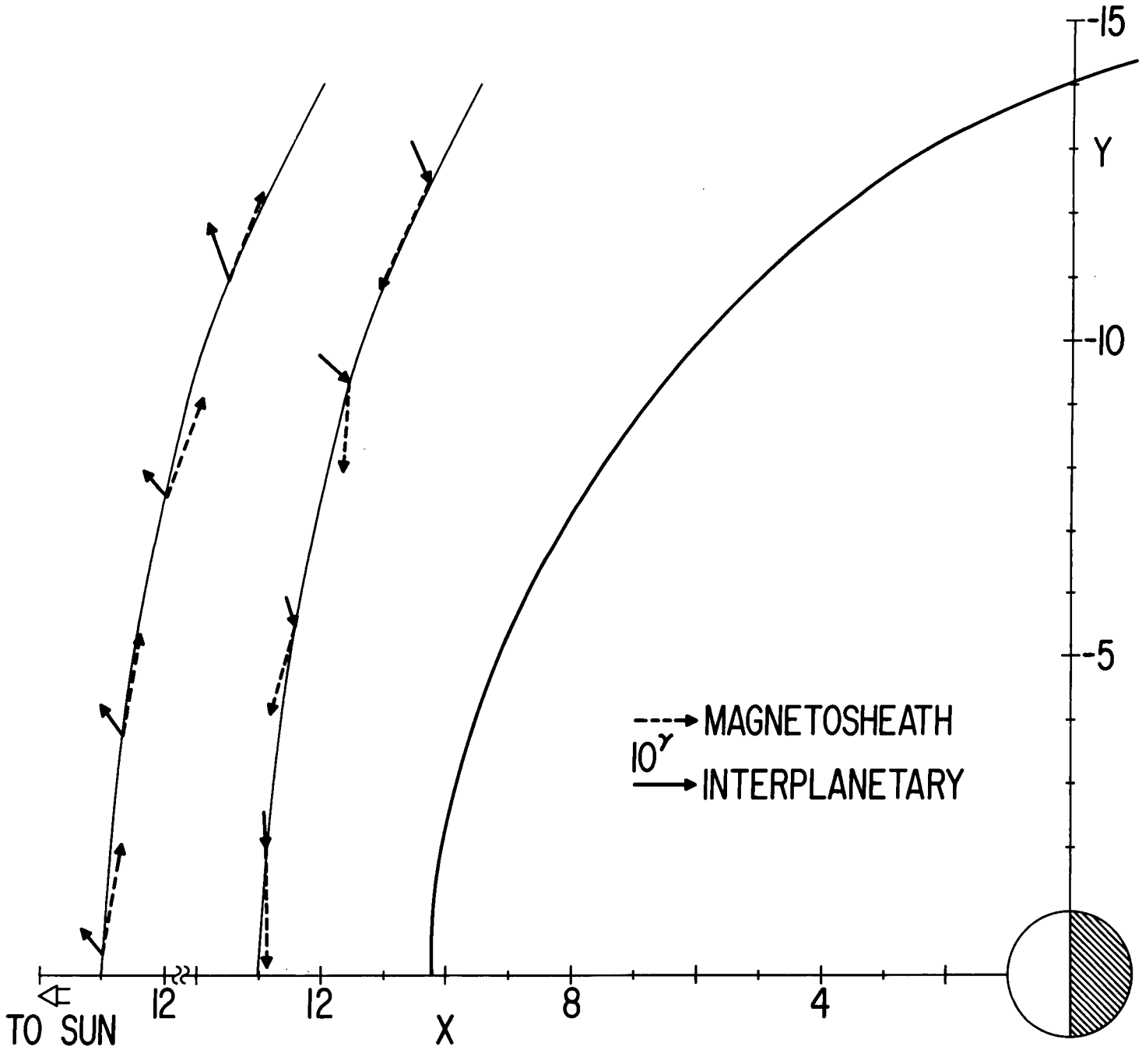

FIGURE 15

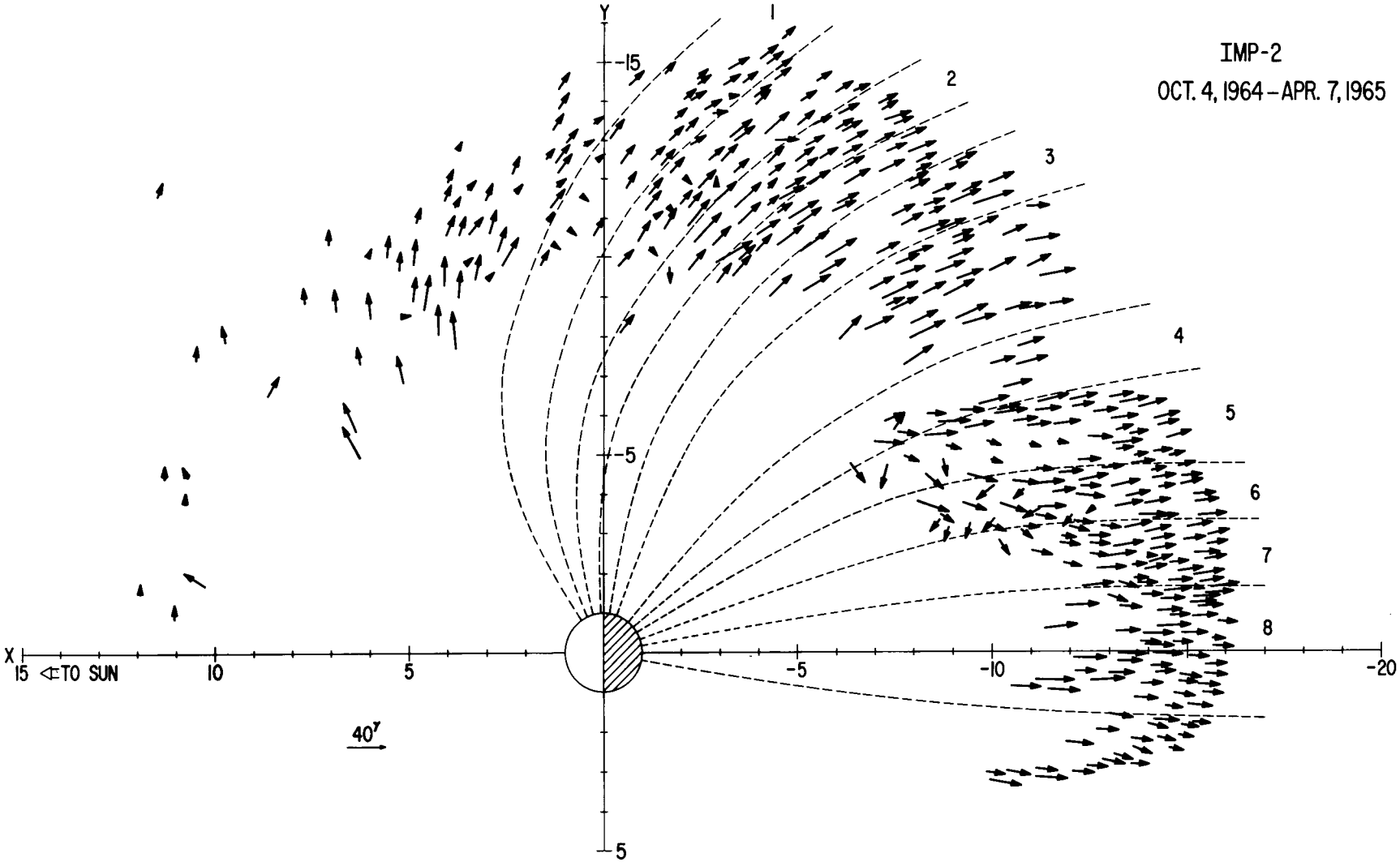

XY SOLAR MAGNETIC PROJECTION

FIGURE 16

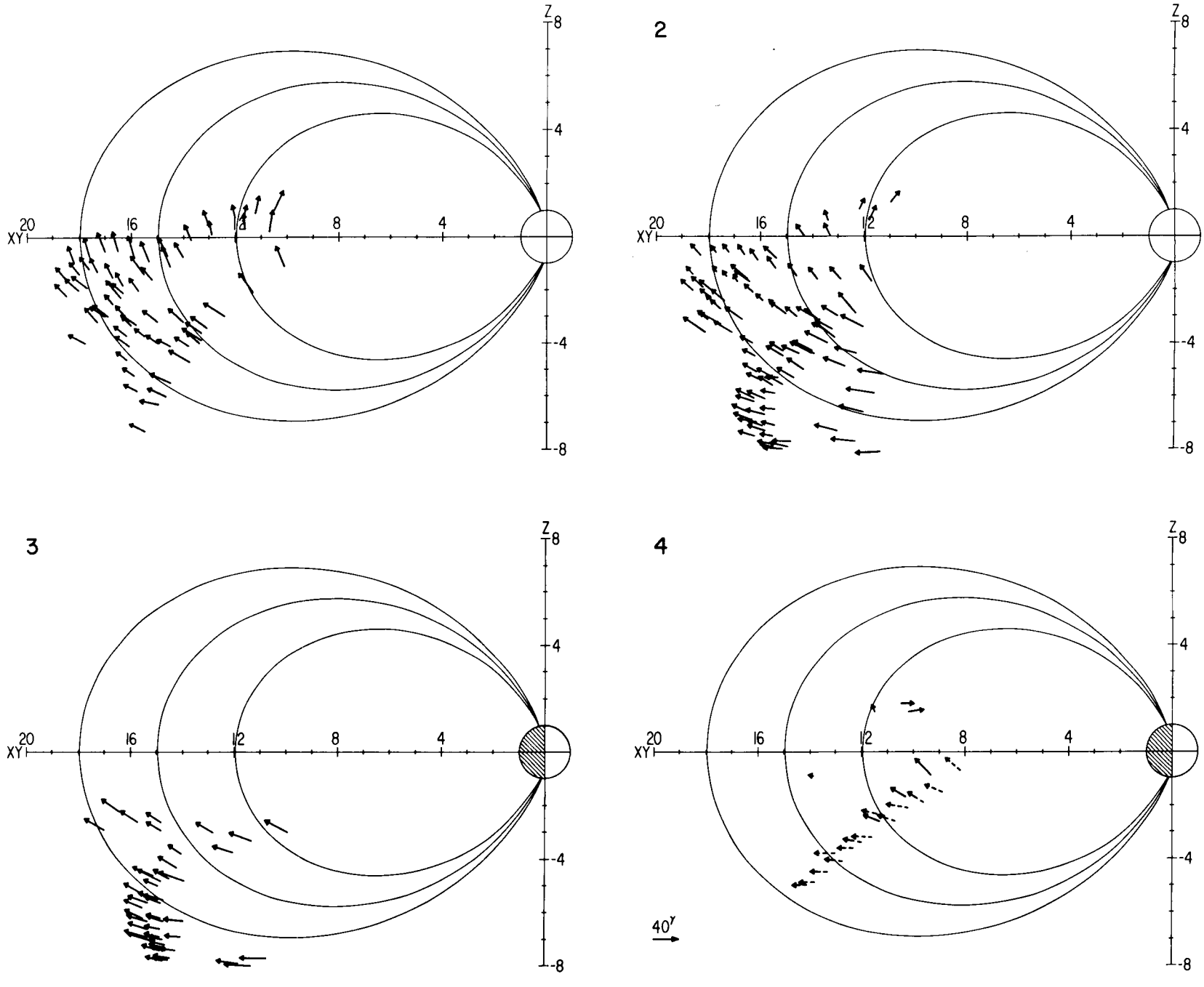

FIGURE 17a

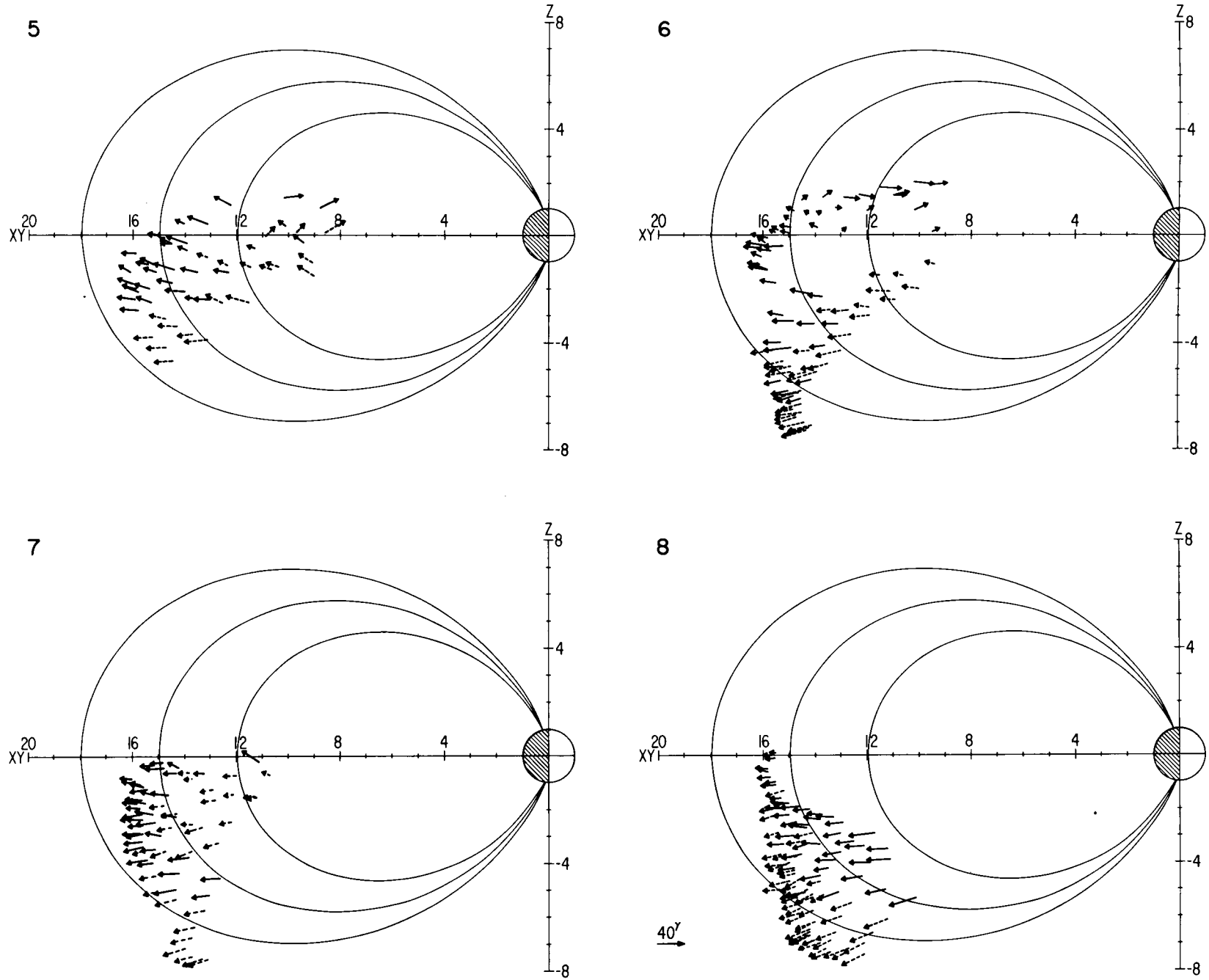

FIGURE 17b